STABILIZED ZrO_2-W COMPOSITES PRODUCED BY UNIDIRECTIONAL SOLIDIFICATION

A THESIS

Presented to

The Faculty of the Division of Graduate

Studies and Research

by

Michael David Watson

In Partial Fulfillment

of the Requirements for the Degree

Master of Science in Metallurgy

Georgia Institute of Technology

December, 1973

STABILIZED ZrO_2 - W COMPOSITES PRODUCED BY UNIDIRECTIONAL SOLIDIFICATION

Approved:

Alan T. Chapman, Chairman

Robert F. Hochman

E. A. Starke, Jr.

NOV. 12, 1973

Date approved by Chairman

ACKNOWLEDGMENTS

The author wishes to express his appreciation to Dr. A. T. Chapman for his advice and assistance in the research and for acting as chairman of the reading committee. Thanks are also expressed to Dr. R. F. Hockman and Dr. E. A. Starke for serving on the reading committee. A special word of thanks is for Mr. W. Ohlinger for the etching and scanning electron microscope work and to Mr. Tom Machrovitch for his help and instruction with practical fabrication techniques in the machine shop.

This opportunity is taken to express the author's sincere appreciation to Dr. Niels Engel for acting as academic advisor and his excellent instruction in many metallurgy courses.

TABLE OF CONTENTS

		Page
ACKNOWLEDGMENTS		ii
LIST OF TABLES		v
LIST OF ILLUSTRATIONS		v
SUMMARY		vii
Chapter		
I.	INTRODUCTION	1
II.	SURVEY OF LITERATURE	4
	Eutectic Structures and Systems The Coupled Zone Theory Induction Heating Stabilization of Zirconia	
III.	EQUIPMENT	23
	Induction Heating Unit Unidirectional Solidification Apparatus	
IV.	PROCEDURE	28
	Pellet Preparation Unidirectional Solidification Sample Examination	
V.	RESULTS	33
	Influence of Frequency Influence of Atmosphere Composition Influence of Growth Rate General Description of the Composite	
VI.	DISCUSSION OF RESULTS	54
	Control of the Internal Molten Zone Composite Microstructure	

TABLE OF CONTENTS (Concluded)

Chapter Page

VII. CONCLUSIONS 71

Appendices

A. CHEMICAL ANALYSIS OF ZIRCOA A-HC ZIRCONIUM DIOXIDE POWDER BY ZIRCORIUM CORPORATION OF AMERICA 73

B. CHEMICAL ANALYSIS OF YTTRIA POWDER BY KERR McGEE CHEMICAL CORPORATION OF AMERICA 74

C. CHEMICAL ANALYSIS OF TUNGSTEN POWDER BY FAIRMOUNT CHEMICAL CORPORATION. 75

BIBLIOGRAPHY 76

LIST OF TABLES

Table — Page

1. Fiber Size, Fiber Density, Composition, and Growth Rate Data for Some ZrO_2-10 Mole Percent Y_2O_3-W Samples 41

LIST OF ILLUSTRATIONS

Figure — Page

1. The Coupled Zone and Equal Saturation Line in a System in which the Extended Liquidus Lines Are Roughly Symmetrical about the Eutectic Point. 8
2. The Liquid-Solid Interface above α and β Lamellae Showing Various Distances and Compositions. 11
3. The Skewed Coupled Zone in Systems with Unsymmetrical Liquidus Lines and the Steps in the Solidification of a Halo. 15
4. The Induction Heating Facilities Used for Unidirectional Solidification of Composites 25
5. Diagram of the Induction Heating Facilities Showing the Position of the Molybdenum Heater when Being Used as a Slow Cooling Post-Heater 26
6. Composite Areas Containing Primary Oxide and Eutectic Structure in ZrO_2 - Mole % Y_2O_3 - 5 Weight % W. 38
7. A Tungsten Dendrite Surrounded by an Oxide Halo and Eutectic Structure in ZrO_2 - 10 Mole % Y_2O_3 - 17 Weight % W. 39
8. The Effect of Growth Rate on Fiber Density in ZrO_2 - Mole % Y_2O_3 - 16 Weight % W. 42
9. The Effect of Varying Growth Rate on the W Fiber Diameter in Y_2O_3 Stabilized ZrO_2-W Samples. 43

LIST OF ILLUSTRATIONS (Concluded)

Figure		Page
10.	Typical Longitudinal Section of a ZrO_2-Y_2O_3-W Pellet Showing the Voids, Unmelted Skin, and the Black Solidified Area	45
11.	Typical Area of Uniform Fiber Growth in ZrO_2-Y_2O_3-W Composites.	46
12.	The Intersection of Three Grain Boundaries or Possibly Colony Walls in ZrO_2-Y_2O_3-W.	46
13.	An Oxide Band in which the W Fibers Renucleate in a Fan Shape.	48
14.	Oxide Bands in which the W Fibers Renucleate Just above the Preceding Fibers	48
15.	Wide Growth Discontinuity or Band Artificially Produced by a Power Fluctuation	50
16.	An Area of W Platelets in a ZrO_2-Y_2O_3-W Sample.	52
17.	The W Fibers Protruding from the ZrO_2-Y_2O_3 Matrix that Has Been Selectively Etched	53
18.	The ZrO_2-Y_2O_3 Matrix with Holes Produced by Selectively Etching Away the W Fibers	53
19.	Schematic Diagram of a Pellet During Unidirectional Solidification	62
20.	Schematic Diagram of the Depression in the Usually Flat Liquid-Solid Interface at a Cell or Grain Boundary	64

SUMMARY

The internal molten zone technique utilizing radio frequency induction heating was developed for unidirectional solidification of Y_2O_3 stabilized ZrO_2-W composites near the eutectic composition. The composites consisted of W fibers aligned parallel in a single phase oxide matrix. The density and size of the W fibers were controlled by the solidification rate with typical values being 11 million fibers of 0.4 micron diameter per square centimeter of composite. The influences of the frequency of induction heating, sample composition, and atmosphere on the initial formation of a stable internal molten zone were studied. The composite microstructure was examined with regard to the effects of composition, atmosphere, and solidification rate. The solidification process was explained using the coupled zone theory for unidirectional solidification of near eutectic melts. Nucleation theories that explain certain solidification phenomena in metal-metal systems were extended to the oxide-metal system, Y_2O_3 stabilized ZrO_2-W.

CHAPTER I

INTRODUCTION

Unidirectional solidification of eutectic alloys has received considerable attention in the past fifteen years. Investigations have progressed from theoretical development to experimental production of composites and in some cases the design and use of the materials for specific applications. The majority of the eutectic compositions that have been studied are metal-metal systems with a few important works in the organic systems. There have been few studies in other types of eutectics such as oxide-oxide mixtures or oxide-metal mixtures. Metal-metal systems have received the most attention because of their potential application in turbine blades and their relatively easy production compared to the oxide systems. Organic systems have been studied because their low melting points have made possible the direct observation and control of the liquid-solid interface. The understanding of the solidification process has been advanced through these studies on organic compositions. Mixtures involving oxides have been avoided due to the refractory problems in containing the molten oxides. The lack of phase diagrams for the oxide-metal systems has contributed to the problems involved in studying this type of eutectic.

The internal molten zone technique was developed for the growth of refractory oxide crystals and later used to study refractory oxide-metal composites. This technique uses radio frequency induction heating to melt the interior of sample pellets while the outer skin of the pellet remains solid and acts as a crucible. Unidirectional solidification of the molten material was achieved by lowering the pellet out of the induction heating coil so that the liquid-solid interface moves up through the pellet.

The first oxide-metal composites unidirectionally solidified using the internal molten zone technique were in the UO_2-W system. The structure consisted of an UO_2 matrix with W fibers or rods aligned parallel to the solidification or growth direction. The W fibers were less than a micron in diameter and the composite had several million fibers per square centimeter. The second oxide-metal system in which unidirectional solidification was achieved was the CaO stabilized ZrO_2-W system. The growth of W fibers in the ZrO_2-CaO-W pellets was restricted to small areas with the majority of the solidified material consisting of dendrites or a degenerate structure.

The purpose of this investigation was to study the factors which affected the solidification process such as composition, growth rate, and atmosphere. To achieve this a method of obtaining a stable molten zone in Y_2O_3 stabilized ZrO_2-W pellets was first developed. Attempts were made to develop a method to achieve uniform solidification of W fibers in the oxide matrix throughout the entire length of unidirectionally solidified material. The knowledge gained from this investigation should advance the understanding of the unidirectional solidification of oxide-metal systems and lead to the solution of several problems in the production of such composites.

CHAPTER II

SURVEY OF LITERATURE

This chapter is a review of the literature related to the topic of unidirectional solidification of Y_2O_3 stabilized ZrO_2-W. Sections include a description of eutectic structures, the systems previously studied and an explanation of the coupled zone theory. The use of induction heating in the internal molten zone technique is briefly explained, and the stabilization of zirconia is reviewed.

Eutectic Structures and Systems

Hogan[1] presents a classification of eutectic microstructures originally developed by Scheil.[2] The structures are divided into three classes, 1) normal, 2) anomalous, and 3) degenerate. Normal structures are those of "highly organized nature" such as lamellar and fiber structures. Anomalous structures have the phases closely intermingled but with much less regularity. Degenerate structures have a minimum association of the phases as if they have solidified completely independently. Normal structures are the most important and are the only structures described here.

The characteristics of the normal eutectic structure as presented by Hogan[1] indicate the phases solidify simultaneously in a close physical association. The solidification takes place by the movement of an almost planear liquid-solid interface. The lamellae or fibers solidify perpendicular to the liquid-solid interface so that each phase is continuous in the growth direction. The spacing of the lamellae or fibers is uniform for any given set of growth conditions. This spacing becomes finer as the solidification rate increases.

Eutectic grains are formed analogous to the grains of a single phase alloy. In these grains each phase has a uniform crystal orientation and grows from a single nucleus. Hogan describes the grains as being two interpenetrating single crystals.

Weart and Mack[3] explain that there are three structures produced during unidirectional eutectic solidification. These are the grain structure, the colony or cell structure, and the eutectic structure, with each one contained in the one preceding it. The grain structure is analogous to the eutectic grains mentioned above in Hogan's nomenclature. Weart[3] states that the colony or cell structure is a "subgrain structure whose units contain several dozen phase particles." ". . .colonies are distinguished by the phase particle arrangement and not by crystallographic orientation as in the case of grains." Weart explains that colonies and grains have been confused in the literature because of the difficulty in differentiating then. The colony structure is best observed in a polished plane which contains the growth direction. The cell boundaries or colony walls will then appear parallel to the growth direction and have the lamellae or fibers curving into the boundary. The third structure is the eutectic structure and refers to the actual shape of the phase particles whether they be lamellar, fiberous, or globular.

The metal-metal eutectic systems have received considerable study, and the majority of the literature and theories on unidirectional solidification are based on metal-metal systems. Kofler[4] and Hunt and Jackson[5] studied organic systems in which the lower melting points made the observation of solidification less difficult. Studies of oxide-metal systems have been limited by experimental difficulties related to high temperatures and the lack of phase diagrams for such systems. Oxide-oxide systems have also received little attention due to the high temperature problems.[6-11] Hogan et al.[12] present a list of 156 different systems which have been investigated.

Investigations of oxide-metal systems have been performed in the School of Ceramic Engineering at Georgia Institute of Technology[13] and at the Metals and Ceramics Division of the Oak Ridge National Laboratory. The UO_2-W system was the first developed at Oak Ridge and has received the most attention.[14-17] The stabilized ZrO_2-W was the second oxide-metal system to be unidirectionally solidified.[18-20] Other systems developed include stabilized HfO_2-W,[21,22] UO_2-Ta, Nb, or Mo,[23] and various rare earth oxides such as Gd_2O_3, La_2O_3, and Nd_2O_3 doped with CeO_2 and Mo or W.[13] Nelson and Rasmussen[24] at Battelle Northwest Laboratory have reported eutectic solidification in the systems Cr_2O_3-Mo, Cr_2O_3-W, and MgO-W. Additional exploratory work at Battelle Northwest invistigating the solubility of refractory metals (W, Mo, Ta, and Re) in numerous molten oxides indicated additional systems may form ordered structures.[25]

Unidirectional solidification of CaO stabilized ZrO_2-W was first reported by Watson.[18,19] The internal zone melting technique was used to melt the interior of cylindrical pellets in an N_2 atmosphere. The frequency for the induction heating was 13.6 megahertz. The solidified interior of the pellets showed three distinct regions. A region of normal eutectic structure was found at the base of the solidified zone. This structure consisted of W fibers parallel to the growth direction solidified in the stabilized ZrO_2 matrix. A second region was a circumferential band adjacent to the unmelted skin containing clear ZrO_2 crystals and no W. The third region was a central area of degenerate eutectic structure containing ZrO_2 dendrites and voids partly filled with $CaWO_3$ and W.

The Coupled Zone Theory

As early as 1922 Brady[26] reported that eutectic structures can be solidified over a range of compositions on either side of the equilibrium eutectic point. This region was termed the "coupled region" or "coupled zone" by Kofler[4] in her investigation of organic eutectic systems. The coupled growth concept was first applied to metallic eutectics by Scheil[2] and later reviewed by Hogan[1,12,27] and used by many other investigators[28-32] to explain the eutectic solidification phenomena.

The coupled zone is a region below the eutectic temperature into which undercooling can lower the temperature of the liquid. Solidification of the melt then produces a normal eutectic structure. The composition range of the coupled region usually includes the equilibrium eutectic composition at all amounts of undercooling but this requirement is not necessary in all cases. If the composition and undercooling of the liquid place the melt in the coupled region, the solidification of both eutectic phases will take place in a coupled manner. This is to say the solidification rates of the two eutectic phases are equal and faster than the solidification rate of any primary phase. If the melt lies outside the coupled region, solidification of one primary phase enriches the liquid in the other component and moves the composition toward the coupled region. Whether the coupled region is reached depends on the nucleation factors involved in the particular system.

The coupled growth theory is based on Scheil's[2] concept that the solidification rate of any solid phase is proportional to the degree of supersaturation of the melt with respect to that phase. If a melt is cooled until it just meets the liquidus line, then it will be just saturated with respect to one phase. A crystal of this phase, if added to the melt, would not grow, but would just be in equilibrium with the liquid. Some amount of supersaturation would be necessary for solidification to take place. This supersaturation of the liquid might be produced by undercooling or by a composition change in the liquid. Scheil[2] states that the rate of solidification increases with the degree of supersaturation according to a parabolic relation.

Hogan[1] describes the most simple ideal eutectic as one in which the liquidus lines are roughly symmetrical about the eutectic point and the volume fraction of the two phases is equal. Figure 1 shows the phase diagram for such a case. The liquidus lines have been extended into the metastable region below the eutectic temperature. Each of these lines represents the composition and temperature at which the supercooled liquid will be just saturated with respect to one of the primary phases. If a melt of the eutectic composition, C_e, is undercooled slightly below the eutectic temperature, T_e, the amount of supersaturation of both α and

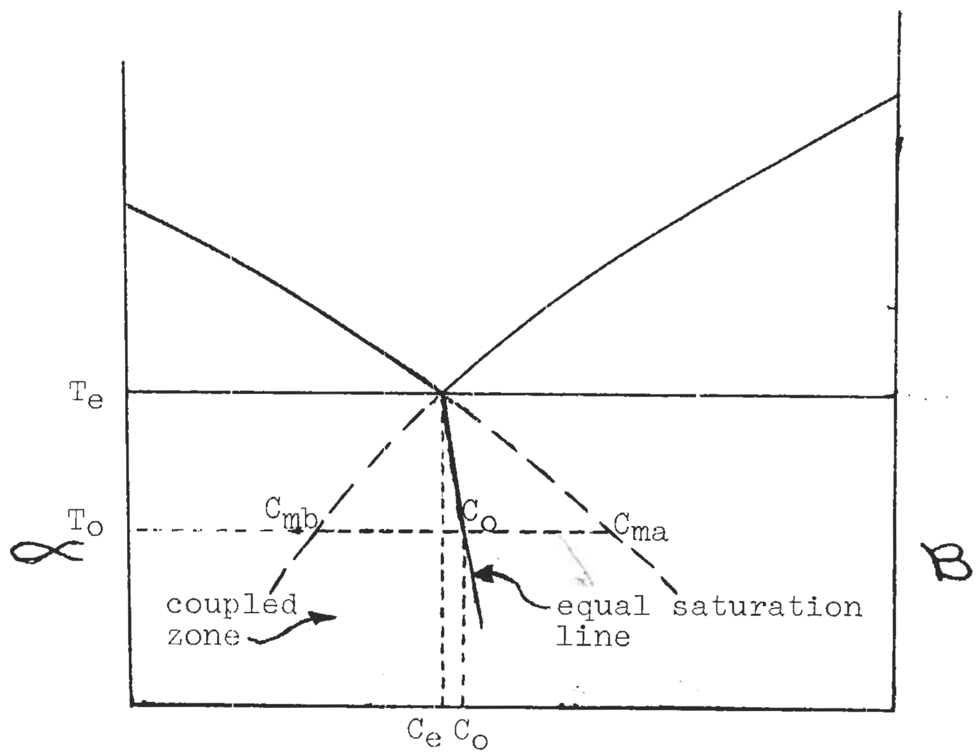

Figure 1. The Coupled Zone and Equal Saturation Line In a System in which the Extended Liquidus Lines Are Roughly Symmetrical About the Eutectic Point. The Distance C_{mb}-C_o Equals The Distance C_{ma}-C_o.

β will be equal. This will cause both phases α and β to solidity together at the same rate in the coupled manner. A flat liquid-solid interface would be the result.

If the liquid is undercooled to a lower temperature, T_o, a different situation develops because of the slight unsymmetry of the extended liquidus lines. To show this, the line from the eutectic point through point C_o is shown in Figure 1 so that the distance $C_{mb} - C_o$ equals $C_{ma} - C_o$. The point C_o represents the melt composition which is equally supersaturated with respect to both α and β at the temperature T_o. The line containing point C_o is drawn so that equal saturation is shown at all temperatures below T_e. This line can then be called the equal saturation line.

If a melt of composition C_e in Figure 1 in which both components have identical diffusion and nucleation properties is undercooled to temperature T_o it will be saturated with respect to α to a greater extent than to β. This is because the distance $C_e - C_{ma}$ is greater than $C_e - C_{mb}$. Both phases can solidify but the α phase will solidify at a faster rate. This causes the solidification of primary crystals of α and moves the liquid composition toward C_o. When the liquid composition reaches C_o both phases will have equal saturation and solidify at the same rate in the coupled manner. The liquid-solid interface will be flat with neither phase leading the other when the liquid composition is on the equal saturation line, the volume fraction of each phase is equal, and the liquidus lines are roughly symmetric.

Coupled growth can be achieved in a region around the equal saturation line by not requiring the liquid-solid interface to be flat.[1] If one phase is allowed to lead the other phase as shown in Figure 2, the growth of the two phases can still be coupled even though the melt composition is not on the equal saturation line. Hogan[1] explains that if the α lamellae solidify at an initially faster rate they will advance ahead of the β lamellae as in Figure 2. The liquid composition in the groove between the lamellae will be C_o (the equal saturation composition) but at the lamellae tips it will be C_α and C_β. At the tip of an α lamella the composition C_α will be depleated of α with respect to C_o due to the solidification of α. This sets up a diffusion of α atoms from the groove of composition C_o to the α lamella tip. Atoms of β are also diffusing from the α lamella tip to the groove. Scheil[2] states this situation will cause the α lamellae to be relatively starved for material compared to the β lamellae. This is because of the longer diffusion distance from the groove to the leading α tips than from the groove to the β tips. This starvation will slow down the α lamella's solidification rate. A rate will be established so that the α and β lamellae will be coupled and the α will lead the β lamella at some specific distance determined by the difference in the liquid composition from the equal saturation composition.

Tiller[33] derived an equation relating the liquid composition expressed as volume fractions to the lead distance of the lamella by starting with the assumption that the flux of solute, β, into the base of the groove of eutectic composition, C_e, from the α lamella must equal the flux of the solute out of the groove to the β lamella. If l_α and l_β are the diffusion distances as in Figure 2 and $\Delta C_i = C_i - C_e$ the equality of

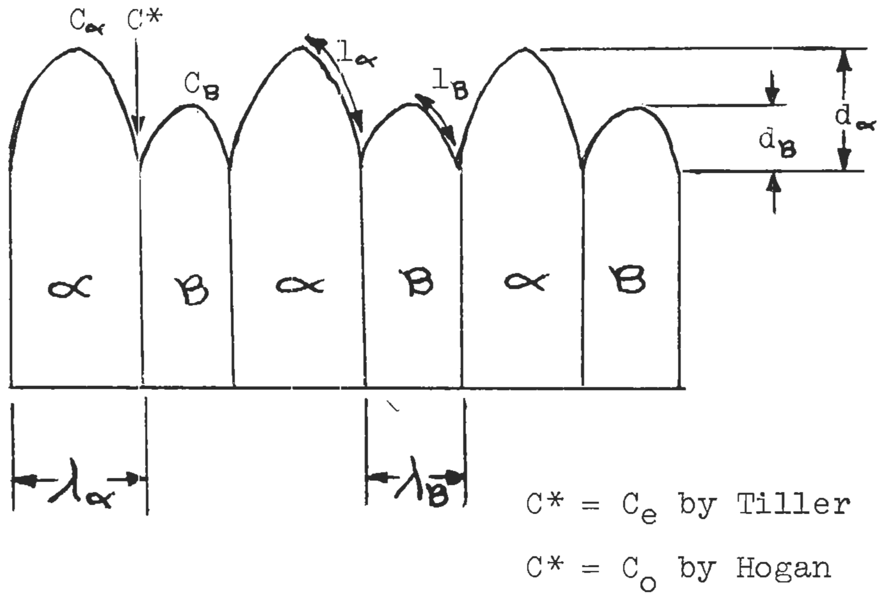

Figure 2. The Liquid-Solid Interface Above α and β Lamellae Showing Various Distances and Compositions.

the fluxes is given by

$$\frac{\Delta C_\alpha}{l_\alpha} = -\frac{\Delta C_\beta}{l_\beta} \tag{1}$$

The Pythagorean theorem is then used to find an approximation for the diffusion distance, l_i, where i represents α or β.

$$l_i = \left\{d_i^2 + \left(\frac{\lambda_i}{2}\right)^2\right\}^{\frac{1}{2}} \tag{2}$$

where d_i and λ_i are defined in Figure 2. Combining these two equations and arranging terms Tiller obtains:

$$\frac{\Delta C_\alpha}{\Delta C_\beta} = -\frac{\lambda_\alpha\left\{1 + \left(\frac{2d_\alpha}{\lambda_\alpha}\right)^2\right\}^{\frac{1}{2}}}{\lambda_\beta\left\{1 + \left(\frac{2d_\beta}{\lambda_\beta}\right)^2\right\}^{\frac{1}{2}}} \tag{3}$$

He then approximates the liquidus lines as being straight lines of slope m_i extending below the eutectic temperature. The compositions C_α and C_β are assumed to be found on these lines at an equal undercooling, ΔT, for both phases. The ratio $\Delta C_\alpha/\Delta C_\beta$ is then related to the slopes by the equation of straight lines

$$\Delta T_i = m_i(C_i - C_e) = m_i \Delta C_i \tag{4}$$

$$\Delta T_\alpha = \Delta T_\beta \tag{5}$$

$$\frac{m_\beta}{m_\alpha} = \frac{\Delta C_\alpha}{\Delta C_\beta} \tag{6}$$

The ratio of lamellar widths, $\lambda_\alpha/\lambda_\beta$, is equal to the ratio of the volume fraction of α phase, V_α, to the volume fraction of the β phase, V_β,

$$\frac{\lambda_\alpha}{\lambda_\beta} = \frac{V_\alpha}{V_\beta} \tag{7}$$

Combining these equations Tiller obtains

$$\frac{V_\alpha}{V_\beta} = - \frac{m_\beta}{m_\alpha} \left\{ \frac{1 + \left(\frac{2d_\beta}{\lambda_\beta}\right)^2}{1 + \left(\frac{2d_\alpha}{\lambda_\alpha}\right)^2} \right\}^{\frac{1}{2}} \tag{8}$$

A similar expression can be obtained by using Hogan's methods which follow the coupled zone theory more closely. He assumes the composition at the base of the groove to be the equal saturation composition, C_o, and the composition, C_α or C_β, at the lamellae tips to be slightly off the extended liquidus line. This slight variation from the composition on the liquidus line provides a supersaturation to drive the solidification process. This has the effect of making $\Delta C_\alpha = - \Delta C_\beta$ which is necessary to have equal solidification rates. So Equation 3 becomes

$$1 = + \frac{\lambda_\alpha \left\{1 + \left(\frac{2d_\alpha}{\lambda_\alpha}\right)^2\right\}^{\frac{1}{2}}}{\lambda_\beta \left\{1 + \left(\frac{2d_\beta}{\lambda_\beta}\right)^2\right\}^{\frac{1}{2}}} \tag{9}$$

which by use of Equation 7 becomes

$$\frac{V_\alpha}{V_\beta} = \left\{ + \frac{1 + \left(\frac{2d_\beta}{\lambda_\beta}\right)^2}{1 + \left(\frac{2d_\alpha}{\lambda_\alpha}\right)^2} \right\}^{\frac{1}{2}} \tag{10}$$

mcw

In Equations 8 and 10 the ratio of the volume fractions, V_α/V_β, is an expression of the melt composition. These equations show how a change in the melt composition from C_e in Tiller's analysis and from C_o in Hogan's analysis can be compensated for by a change in the lamella lead distance and lamella widths. These changes effect the diffusion distances so that the solute fluxes can remain equal. Equations 8 and 10 actually say that coupled growth can be obtained at any composition if the lead distance is great enough. But there is a limit to the lead distance which defines the boundaries of the coupled zone. If the lead distance is too great the leading phase will grow laterally and become dendritic. Several studies have been made on this eutectic to dendritic translation in metal-metal systems.[32, 34-36]

Figures 1 and 3 show two possible types of coupled regions as described by Kofler.[4] The shaded areas show the coupled region in which the eutectic structure can be solidified. Figure 1 has the liquidus lines almost symmetrical about the eutectic point. In such a case the eutectic structure can easily be obtained in any composition near the eutectic composition if enough undercooling can be achieved. Figure 3 represents the situation where the liquidus lines are very unsymmatrical. The coupled zone is no longer centered below the eutectic point, but skewed toward the component with the higher melting point. Chadwick[29]

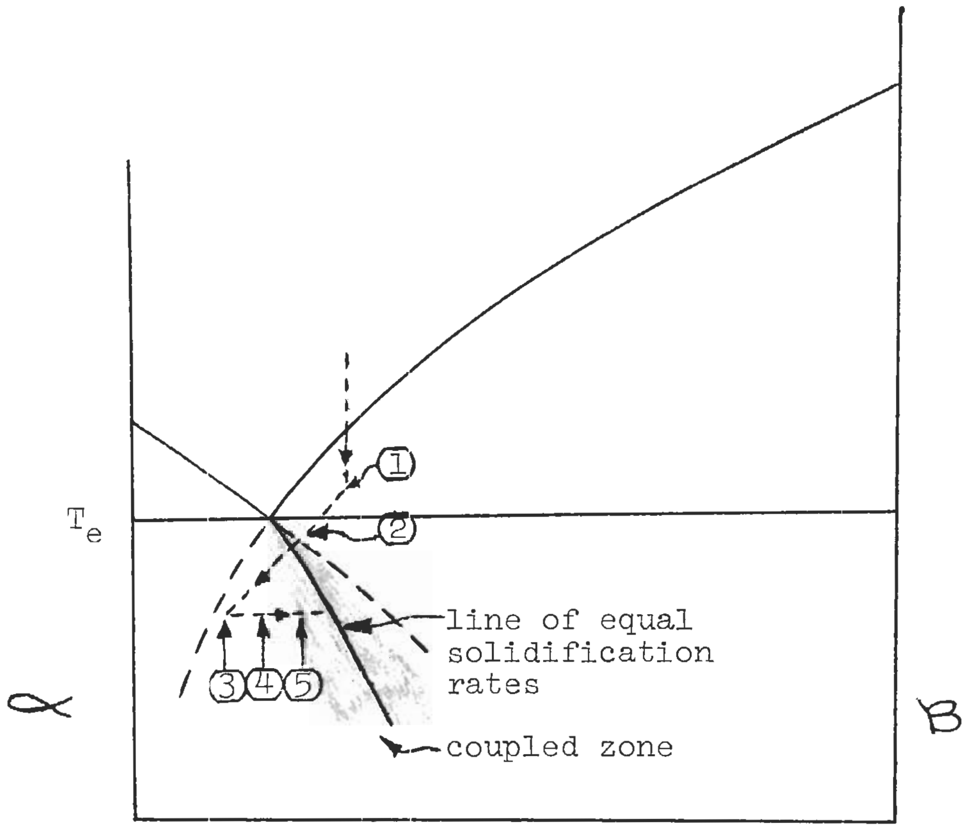

1 nucleation of β phase
2 growth of β dendrite
3 nucleation of α phase
4 growth of α halo
5 nucleation of β on the halo and growth of eutectic

Figure 3. The Skewed Coupled Zone in Systems with Unsymmetrical Liquidus Lines and the Steps in the Solidification of a Halo.

states the reason for this is that the supercooling of the liquid is relatively much greater for the phase with the higher melting point. The temperature dependence of solidification rate of this phase is much greater than for the low temperature melting phase. With a given amount of undercooling below the eutectic temperature, one phase is cooled below the melting point of the pure component much greater than the other phase. This causes unequal solidification rates even if the melt is equally supersaturated with both phases. This inequality of solidification rates at equal supersaturation produces the displacement of the coupled zone to a region in which the rates are equal. The coupled zone is actually centered about a line of equal solidification rates. This line corresponds to the equal saturation line when the components have similar melting points or the liquidus lines are symmetrical about the eutectic point.

Hogan[37] uses the skewed coupled zone and nucleation factors to explain the solidification of "halos" around primary dendrites. Sundquist et al.[38] describe the halos as a secondary phase surrounding the primary phase. The explanation of halo formation is based on nucleation theory presented by Sundquist and Mondolfo.[39] They state that metals that are difficult to nucleate have complex or open structures and are good nucleating agents for other metals. Similarly metals that are easy to nucleate have simple structures and are poor nucleating agents for other metals. In eutectic solidification Sundquist[38] states that only one phase acts as the nucleating agent for the eutectic structure on both sides of the eutectic composition.

Figure 3 illustrates the solidification of halos as described by

Davies,[28] Hogan,[37] and Sundquist.[38] The primary phase, β, nucleates and grows dendritically moving the liquid composition toward the coupled zone. If the secondary phase, α, is difficult to nucleate due to insufficient undercooling or to the β phase being a poor nucleating agent the liquid composition could move across the coupled zone. When the liquid composition has crossed the coupled zone and is highly supersaturated with α this phase will nucleate. Since the liquid composition is in a region in which α has the greater solidification rate, a halo of α will solidify around the dendrite. The liquid composition will then move back toward the coupled zone again. Since the β phase is easy to nucleate the eutectic structure can start solidifying with the α lamella continuous with the halo and the β phase nucleating on the halo. Further solidification produces only the eutectic structure.

With the skewed coupled region, if the melt has the eutectic composition or is richer in α, β dendrites and α halos could still form if the β phase is much easier to nucleate. The melt must be supercooled below the eutectic temperature without the nucleation of the α phase. The β phase then might nucleate first and grow a dendrite even though the α phase should be the primary phase if equilibrium conditions were met. This enriches the liquid in α and at some large degree of supersaturation the α phase nucleates. The solidification of the α phase as a halo then moves the liquid composition back toward the coupled region.

Explanations of anomalous eutectic structures especially in the Al-Si system[31] are based on the skewed coupled zone.[12,29] The solidification steps can take many possible paths depending on the precise differences in solidification rates and nucleation properties. Generally the solidification is similar to the last case described above but repeated nucleation of both phases and large differences in solidification rates prevents the liquid composition from reaching the coupled region, and an anomalous structure is produced in which the phases do not solidify simultaneously nor are the phases continuous.

The coupled zone theory successfully explains the solidification of a normal eutectic structure. The solidification of eutectic structures from melts not of the eutectic composition and the formation of halos around primary dendrites can be explained by the theory. The coupled zone theory gives a good qualitative understanding of the solidification process involved in the growth of composites.

Induction Heating

A modified floating-zone technique has been used for melting and controlled solidification of refractory oxides and oxide-metal composites.[13,14,40-42] This technique employs radio frequency (rf) induction heating in the range 4 to 30 megahertz. Oxide pellets are preheated to an elevated temperature at which they have sufficient electrical conductivity to support eddy current heating. The input power is balanced against the high radiant heat loss from the pellet surface at a level sufficient to melt the interior of the pellet. If the pellet material has a high enough melting point to allow a large radiant heat loss and a low thermal conductivity, the interior can be molten while the surface remains unmelted. This unmelted skin then acts as a crucible eliminating a source of contamination. For growing crystals or composites, the induction heating method has the following advantages:

1. Heat is generated within the sample.

2. There is no contact required between the sample and external containment pieces.

3. Very high temperatures can be reached in a short period of time.

4. The heating can be restricted to localized areas.

5. Control of the atmosphere is simple.

Induction heating depends on the eddy currents established in the work piece. The current distribution of these eddy currents decreases exponentially from the surface to the interior of a cylindrical work piece. This is known as the skin effect in induction heating. A "skin depth" is defined as the depth below the surface at which the current density has been reduced to 1/e or about 37 percent of the surface current density.[43] The ratio of the radius of the work piece to the skin depth must exceed four or five to achieve sufficient efficiency in heating the piece. Gayet[44] gives an equation,

$$D = \frac{1}{2\pi}\sqrt{\frac{10^9}{f\,\sigma}} \tag{11}$$

for the skin depth, D, in centimeters where f, the frequency in hertz, and σ, the electrical conductivity in (ohm-centimeters)$^{-1}$. Any increase in frequency or conductivity decreases the skin depth and increases the heating efficiency. Gayet calculated for a 3.5 cm diameter UO_2 pellet the frequency would have to be about 10^{10} hertz to have efficient heating at room temperature. He then calculated that using a five megahertz frequency and preheating the UO_2 to 1300°C to increase the conductivity, the efficiency would be sufficient to melt the oxide. Since frequencies above about 30 megahertz are difficult to contain without arcing problems, the oxide's conductivity must be increased by preheating.

Stabilization of Zirconia

Pure ZrO_2 undergoes a reversible polymorphic phase transformation at about 1000°C. This phase transformation is accompanied by a large discontinuity in the thermal expansion which causes severe cracking or destruction of any piece made from pure ZrO_2. To overcome this problem, ZrO_2 is reacted with other oxides to stabilize the resulting solid solution in a crystal structure which does not undergo any disruptive phase change.

From room temperature up to about 1000°C pure ZrO_2 is monoclinic. The exact transformation temperature is not known, but above about 1000°C the tetragonal crystal structure is stable. Both of these crystalline forms are slightly distorted cubic structures of the CaF_2 type. Smith and Cline[45] have verified the existence of a face centered cubic form stable above 2285° ± 15°C. The crystal structure of ZrO_2 can be changed by additions of oxides such as MgO, CaO, MnO, TiO, and Y_2O_3. This results in a cubic solid solution which is stable throughout the temperature range.

Roth[46] lists a general set of rules for reactions of ZrO_2 with other binary oxides. Reactions of ZrO_2 with oxides containing smaller divalent ions such as with MgO, CaO, MnO, and TiO, result in the stabilized cubic solid solutions. Exceptions to this are BeO and ZnO. Oxides containing larger divalent ions form 1:1 perovskite type compounds. The Ca^{+2} ion is intermediate in size and forms a solid solution in small amounts but forms a compound in equal molar mixtures. Reactions with oxides of smaller trivalent ions such as with Y_2O_3 and In_2O_3 form cubic solid solutions. The smallest trivalent ion Al^{+3} is an exception. Larger trivalent ions in La_2O_3 and Nd_2O_3 result in $A_2B_2O_7$ type compounds along with solid solutions. Smaller tetravalent ions such as in SiO_2 and TiO_2 result in 1:1 compounds, but larger tetravalent ions such as in UO_2 and CeO_2 result in tetragonal solid solutions.

A previous investigation[18,19] used CaO_2 to stabilize ZrO_2 for unidirectional solidification with W. The central area of the pellets contained dendrites of ZrO_2 and voids containing $CaWO_3$ and W. The formation of the $CaWO_3$ complicated the solidification process and may have led to the dendritic growth. A survey of the other stabilizing oxides revealed that yttria, Y_2O_3, does not form compounds with W nor ZrO_2. On this basis, yttria was chosen as the stabilizing oxide to use with ZrO_2 in this investigation.

Duwez et al.[47] studied the phase relationships in the ZrO_2-Y_2O_3 system. They found in the range of zero to five mole percent Y_2O_3 that the temperature for the tetragonal to monoclinic transformation is lowered from 1000°C to about 400°C. In the range 7 to 55 mole percent Y_2O_3, a cubic solid solution was found stable at 2000°C. At 1375°C they found this cubic solid solution region shifted only slightly to lower Y_2O_3 compositions. They presented a phase diagram of the system showing the cubic solid solution region extending from room temperature to the melting point over the composition range at room temperature of 7 to 45 mole percent Y_2O_3. Solidification of oxide mixtures in this range would avoid the disruptive phase transformation seen in pure ZrO_2.

Carniglia et al.[48] report ZrO_2 is slightly non-stoichiometric at temperatures above $1000^{\circ}C$. At high temperatures and oxygen pressures below one atmosphere the ZrO_{2-x} is oxygen deficient and black in color. The dark color is due to free electrons in the oxygen vacancies. Stoichiometric ZrO_2 is white in polycrystalline form or clear as single crystals. Carniglia reported the ZrO_{2-x}-Zr phase boundary was located at $ZrO_{1.986}$ at $1800^{\circ}C$ and an oxygen pressure of 3.5×10^{-6} atmospheres.

CHAPTER III

EQUIPMENT

The equipment used for producing stabilized ZrO_2-W composites consisted of a Lepel high frequency induction heating unit and the associated apparatus for control of the unidirectional solidification. Since this equipment is vital in the production of the composites it will be described in detail. Other equipment used for pellet preparation and examination of the composites is less important and will not be discussed in this chapter.

Induction Heating Unit

A Lepel high frequency generator, model number T-10-3-DF1-E-HW, type T-1003-58, serial number 7023 was used to supply power for the induction heating. This generator is the vacuum tube oscillator type, rated at 10 kilowatt output, capable of operating in the frequency ranges of 2.5 to 8 megahertz and 15 to 35 megahertz. The proper selection of coils and capacitors that can be interchanged within the unit determines the frequency of operation. A variable grid coil capable of adjustment during operation made possible a fine tuning of the unit to match the work load being heated. Meters on the generator's control panel showed the filament voltage, grid current, plate current, plate voltage, and control current. The plate current and voltage were used to record and control the power settings used.

The work load consisted of a load coil and the material to be heated. The load coil was constructed from "flat" copper tubing of rectangular cross section 1/8 inch by 1/4 inch. The coil was a 6 and 1/2 turn helix with a 1 and 3/4 inch inside diameter and 2 and 1/2 inches long. Connections in the generator supplied cooling water which circulated through the coil.

Unidirectional Solidification Apparatus

The facilities in addition to the Lepel generator for oxide metal composite growth were developed as part of this investigation and other research being done concerning composite growth. The growth facility shown in Figure 4 was mounted on a table that could be manually raised or lowered by means of a crank. Mounted below the table were an hydraulic cylinder for sample movement and a vacuum pump. On the side of the table were the controls for the hydraulic system and atmosphere.

Figure 5 shows a schematic diagram of the growth facilities mounted on the table. A brass support held a silica tube for containing the atmosphere. A ceramic support held the molybdenum preheater tube. A steel shaft extended from the hydraulic cylinder up through the table, the brass support, and the preheater tube. On the end of the steel shaft was an alumina tube used to support the sample. Movement of the table raised or lowered the silica tube and preheater tube independent of the steel shaft and sample. Movement of the sample was accomplished by the hydraulic cylinder. A system of needle and shut off valves controlled the flow of the hydraulic fluid so that the sample could be either raised or lowered. Controlled rates in the range from near zero up to about

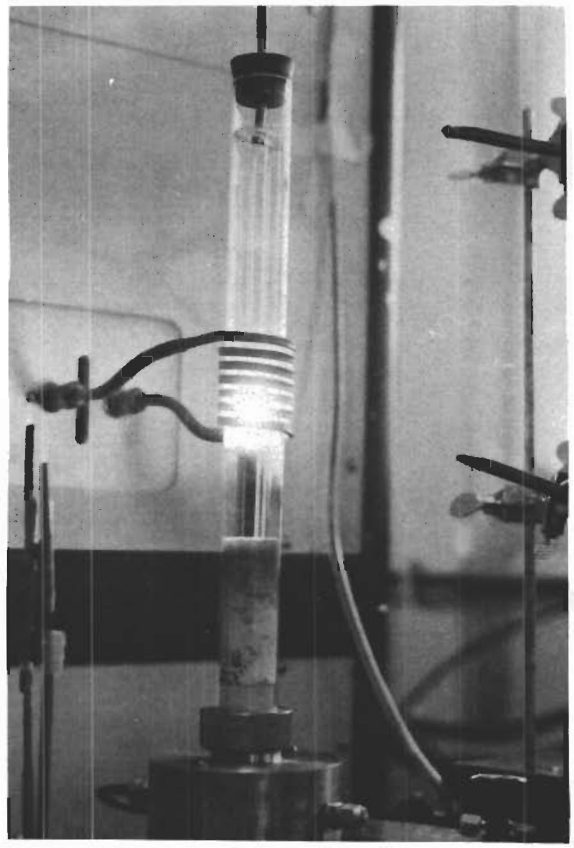

Figure 4. The Induction Heating Facilities Used for Unidirectional Solidification of Composites. A Hot Sample Is Just Above the Molybdenum Tube in the Induction Coil.

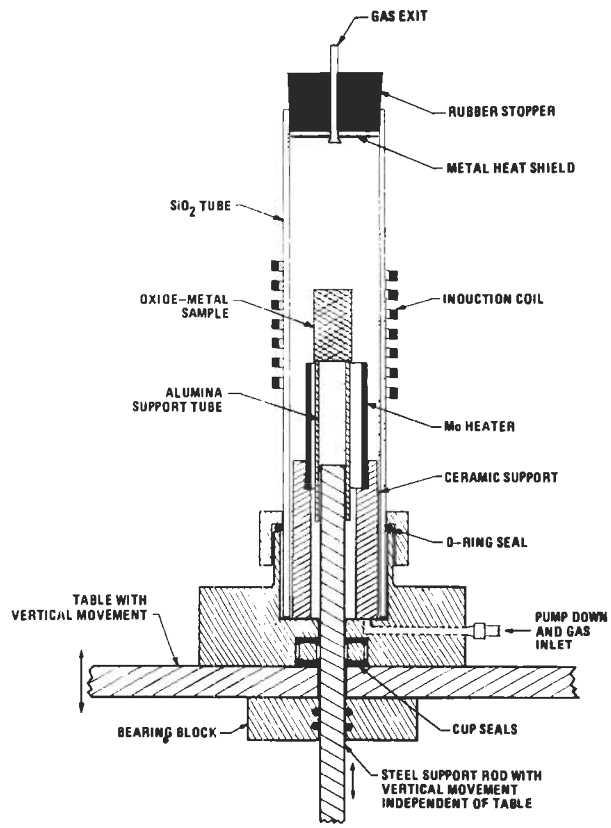

Figure 5. Diagram of the Induction Heating Facilities Showing the Position of the Molybdenum Heater When Being Used As a Slow Cooling Post-Heater. The Sample Pellet Would Be Slowly Lowered into the Molybdenum Tube.

twenty centimeters per hour could be achieved.

Control of the atmosphere was accomplished by the use of a vacuum pump, nitrogen and hydrogen tanks, flow meters, and bubble bottles. The vacuum pump was used to pump down the system to about 50 millitorr and to check for major leaks. The gases to be used passed through flow meters, were mixed, and entered the silica tube through the brass base. After exiting the silica tube at the top, the gas passed through a filter to trap airborne solids which would foil the vacuum shut off valve. The gas finally went through bubble bottles which prevented back streaming of any air into the system.

CHAPTER IV

PROCEDURE

This section will explain in detail the general procedures used for producing stabilized ZrO_2-W composites. Since the investigation involved studying the factors that influenced the growth of these composites many of the procedures were necessarily varied according to the objectives of the experiment. Consequently, only the general procedure that eventually evolved as giving the best results is described. Details of procedural variations and the effects of various changes are given in the results section.

Pellet Preparation

The preparation of sample pellets for internal melting and unidirectional solidification was carried out in three steps: (1) the wet mixing of the ZrO_2 and the Y_2O_3 stabilizer in batches of several hundred grams, (2) the dry mixing of the tungsten and oxide power mixture for each separate pellet, and (3) the pressing of the powder mixture to form a pellet.

Sources for the materials used were as follows: Zirconia powder, A-HC, minus 325 mesh, from the Zirconium Corporation of America, Solon, Ohio. Yttria powder, code 1116, from Kerr McGee, West Chicago, Illinois. The tungsten powder was obtained from two sources, Fairmount Chemical Corporation and Fisher Scientific, purified t-363.

The wet mixing of the oxides was done in batches typically of 600 grams. The calculated amounts of each oxide were weighed on an analytical balance and placed in an electric blender. Enough distilled water was added to make a fluid mixture and then it was mixed for five minutes. The mixture was then dried overnight, crushed in a mortar and pestle, and then passed through a 60 mesh screen.

For each individual sample pellet the amount of tungsten to be added to the oxide mixture was calculated and weighed on an analytical balance. The oxide and tungsten powders were then placed in a glass jar and shaken vigorously for five minutes.

To form a pellet the oxide-tungsten powder mixture was dry pressed at 23,000 psi in a 3/4 inch diameter steel die using an hydraulic press. This produced a pellet 3/4 of an inch in diameter, typically 1/2 inch long, and weighing 50 grams.

Unidirectional Solidification

The process of producing a unidirectionally solidified composite from the oxide-tungsten pellets consisted of a preheat period, coupling directly to the pellet, establishing a stable molten zone, unidirectional solidification, and a cooling period. Control of temperature in this process was critical but the reading of accurate temperatures using an optical pyrometer was prevented by vapor deposites forming on the silica tube. All temperatures given are as read surface temperatures, uncorrected for emissivity and absorption. Control of the process was achieved by careful control of the power settings of the Lepel generator. The necessary power settings varied with the sample composition, atmosphere, and position of the pellet in the coil. These power settings are reported in the results section. Typical temperatures will be reported here in the procedure for clarity.

The set up and preheat procedure was as follows: the sample pellet was placed on the Al_2O_3 support tube as shown in Figure 5. Careful adjustments were made to be sure the pellet, molybdenum preheat tube, silica tube, and induction coil were all concentric. The system was pumped down to about 50 millitorr pressure and then filled with the gas to be used as an atmosphere. Nitrogen, hydrogen, or mixtures of the two gases were used as a dynamic atmosphere flowing at about 500 cc per minute. With the preheater tube raised around the sample, the temperature was then slowly increased to about 1600°C.

After the desired preheat temperature was reached the sample pellet was then coupled to with the rf field to allow additional induction heating. This was accomplished by turning the power to a minimum, quickly lowering the preheat tube well out of the induction coil, and turning the power to a maximum. The sample pellet was then exposed to the rf field and eddy currents established which caused additional heating. After 10 to 30 seconds the interior of the pellet melted, causing a change in the load seen by the Lepel generator. This caused a sudden simultaneous decrease in the plate voltage and an increase in the plate current. At this point the power was quickly cut back to prevent the molten interior from melting through the outer skin which was at about 1850°C. Adjustments were made on the generator's grid current and plate current to bring them to the desired settings and the pellet was allowed to equilibrate for five minutes before proceeding.

Unidirectional solidification was achieved by lowering the pellet through the induction coil. Variations in the lowering rate were examined as one of the factors effecting composite growth. When experiments were not concerned with the lowering rate, a rate of approximately two centimeters per hour was used. After the hot molten zone had traveled to the top of the pellet, additional lowering caused the pellet to decouple from the rf field. This caused a sudden cooling of the pellet when the molybdenum tube was not being used as a postheater for slow cooling.

If a slow cooling of the sample after solidification was desired, the molybdenum tube was then raised into the lower turns of the induction coil, as shown in Figure 5. This caused the upper portion of the tube to be about $1500^{o}C$ and kept the sample hot as it was lowered out of the induction coil. Additional adjustments were made to the Lepel generator's grid and plate currents and another five minutes was allowed for the system to equilibrate.

Sample Examination

Sample examination was mostly done by metallographic techniques. Pellets were usually cut in half parallel to the lowering direction using a diamond saw. The samples were ground flat using SiC abrasive papers (180, 320, and 600 grit) and then polished on a nylon covered wheel with one micron diamond paste. A Reichert MeF metallograph equipped for dark field as well as normal bright field viewing was used for taking photomicrographs. In dark field viewing the fibers slightly beneath the surface were visible while bright field viewing showed only the surface features.

Scanning electron microscope (SEM) examination was used for determining fiber diameters and densities. Thin slices of the composite were cut normal to the fibers, polished as above, and then etched in boiling phosphoric acid for 14 hours before examination in the scanning electron microscope. SEM plots were then used to determine diameters and count the density of the fibers.

CHAPTER V

RESULTS

The major areas investigated controlling the growth of Y_2O_3 stabilized ZrO_2-W composites were the influence of frequency upon establishing a stable molten zone, the determination of the composition giving the best composite growth, the influence of growth atmosphere, and the effect of the growth rate on the oxide-metal composite structure. The results will be reported in separate sections for each topic. In the case of composition and atmosphere there is some overlapping of these because the atmosphere effects the composition needed to produce optimum growth. Also, a section is included describing the various details of the composite produced.

Influence of Frequency

The induction heating frequency is one of the most important factors in the establishment and control of an internal molten zone. Frequencies of 16, 7.6, and 3.6 megahertz were used to establish stable molten zones. Initially the highest frequency, 16 megahertz, was used because it was known that direct coupling and subsequent induction heating in the stabilized ZrO_2-W could be established more readily at the higher frequencies. Reduction of the frequency to 7.6 and then 3.6 megahertz was done to reduce arcing and increase the penetration of the rf field into the pellet. After 3.6 megahertz was found to be satisfactory, this frequency was used for all the remaining experiments.

When using 16 megahertz the ZrO_2-W samples could easily be induction melted but control of the molten zone was difficult. The sample pellet was preheated to about 1600°C using a plate current at 0.80 amp and plate voltage of 7.1 kilovolts. After coupling, power settings of 1.10 amps and 3.7 kilovolts produced a surface temperature of about 2200°C. In all experiments using 16 megahertz the molten interior melted through the thin solid skin spilling some of the molten material. In the solidified regions of the samples there were always many small voids. Arcing from the induction coil to the silica tube and sample was a major problem in many experiments if the growth equipment and sample were not lined up perfectly. This frequency was abandoned due to the spilling of the molten interior and arcing problems.

In an effort to increase skin thickness the frequency was lowered to 7.6 megahertz. The arcing problem was eliminated at this frequency but there was still the problem of preventing melting through the skin. This frequency was abandoned to try 3.6 megahertz after several experiments failed to establish control of the molten zone.

At 3.6 megahertz there were minimum arcing problems and careful control of the power settings prevented spills. This frequency was established as the frequency to use in further experiments. For a ZrO_2-10 mole percent Y_2O_3-16 weight percent W composition melted in a N_2-H_2 gas mixture, the power settings used were 0.58 amp and 3.8 kilovolts. With higher power settings the molten material melted through the skin. If the power was slightly lower the solidified area contained many small voids. Control of the power settings within very narrow limits (which differed for each composition) was necessary to prevent spills of molten material or the formation of voids in the solidified composite. Other than the close control necessary, this frequency was suitable for control of the molten zone and consequently, the growth of good composite samples.

Influence of Atmosphere

Atmospheres of nitrogen or hydrogen or mixtures of these gases were used for composite growth. The noble gases were not used because the high frequency field caused gas plasmas and resulted in arcing problems. Oxidizing atmospheres could not be used because of the oxidation of the tungsten or molybdenum tubes. The type of atmosphere greatly affected the optimum composition used to produce the composites. These results are reported in the composition section.

When pure nitrogen was used for the growth atmosphere, there was considerable vapor deposition of a black or dark brown material on the silica tube. This prevented observation of the sample and led to slight arcing problems as the deposit became thicker with time during long experiments. X-ray analysis found this deposit to be a mixture of W, WO_2, and WO_3.

If a mixture of 90% N_2 and 10% H_2 was used as the atmosphere, the vapor deposits were reduced considerably. With this atmosphere the deposits were so small that they produced no major problems. Most of the experiments on composite growth were then done using the mixture of nitrogen and hydrogen.

An atmosphere of pure hydrogen resulted in a minimum of vapor deposits. Only a very small amount of orange-brown condensate formed just after melting the sample pellet. The hydrogen atmosphere also cooled the sample or preheater tube more than the nitrogen atmosphere. This made slightly higher power settings necessary to produce the same temperature. Power settings for solidification of a ZrO_2-10 mole percent Y_2O_3-6.5 weight percent W sample in H_2 were 0.65 amp and 4.4 kilovolts.

Composition

Two composition variables investigated were the Y_2O_3 stabilizer content and the W metal content. Only two variations in the Y_2O_3 content were investigated but a series of experiments employing different W contents were necessary to establish the optimum W addition to the Y_2O_3 stabilized ZrO_2.

A single phase region is reported in the ZrO_2-Y_2O_3 system which extends from 7 to 56 mole percent Y_2O_3. Solidification of compositions in this region was desired because this stabilized a cubic structure that does not have any disruptive phase transformations as seen at the lower Y_2O_3 contents. A composition containing 7.9 mole percent Y_2O_3 was selected for the first experiments. Good composite growth was produced but the pellets were badly cracked even when slow cooling methods were used. An increase of the Y_2O_3 content to 10 mole percent was made on the suspicion that some of the Y_2O_3 may have vaporized and moved the composition out of the cubic phase region. Good composite growth was again achieved but there was no improvement in the cracking problems. Higher Y_2O_3 contents were tried but abandoned because of increasing difficulty in induction coupling to the material. No significant difference was seen in the quality of the composites produced in the 7.9 or 10% Y_2O_3 compositions but there was a variation in the amount of W necessary to produce the best samples.

The W content was found to have a considerable effect on the fiber growth. An optimum W content was established which would give the greatest area of uniform fiber growth. In samples containing 7.9 mole percent Y_2O_3, the best tungsten content was 10 weight percent W when solidified in the 90% N_2 - 10% H_2 atmosphere. This produced a pellet with good fiber growth throughout most of the pellet except for the upper portion of the solidified area which contained some areas of primary oxide. Figure 6 shows a typical area of this primary oxide growth. Additions of 5% W produced much larger areas of primary oxide in the pellet. Additions of 15% W produced W dendrites within the fiber area and still contained primary oxide in the upper portion of the pellet.

Increasing the Y_2O_3 content to 10 mole percent required 16 weight percent W to achieve the best eutectic growth when solidified in the 90% N_2 - 10% H_2 atmosphere. Although the pellets containing 10% Y_2O_3 and 16% W had extensive areas of uniform fiber growth, some primary oxide was also present in the upper portion of the sample. If 15 weight percent W was used, the area of primary oxide in the upper portion of the pellet was noticeably larger. This effect was even greater when 12 or 10% W additions were made. When 17% W was used dendrites of W occurred in the fiber area and there were still small areas of primary oxide in the upper portion of the pellet. Figure 7 shows the effects of such W dendrites on the fiber growth.

During the solidification of stabilized ZrO_2-W samples in the 90% N_2 - 10% H_2 atmosphere, the composition of the eutectic material does not

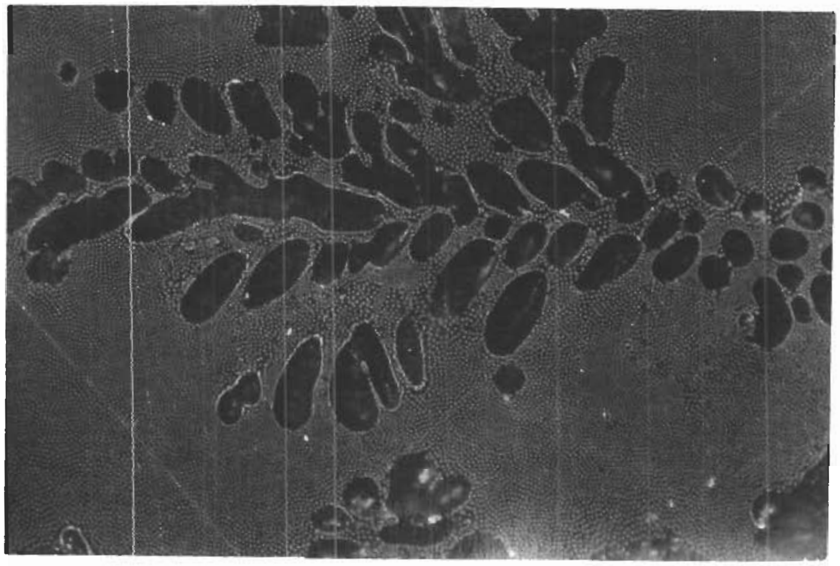

a) Transverse Section, Growth Direction Is Normal to Polished Plane. Dark Field, 200X

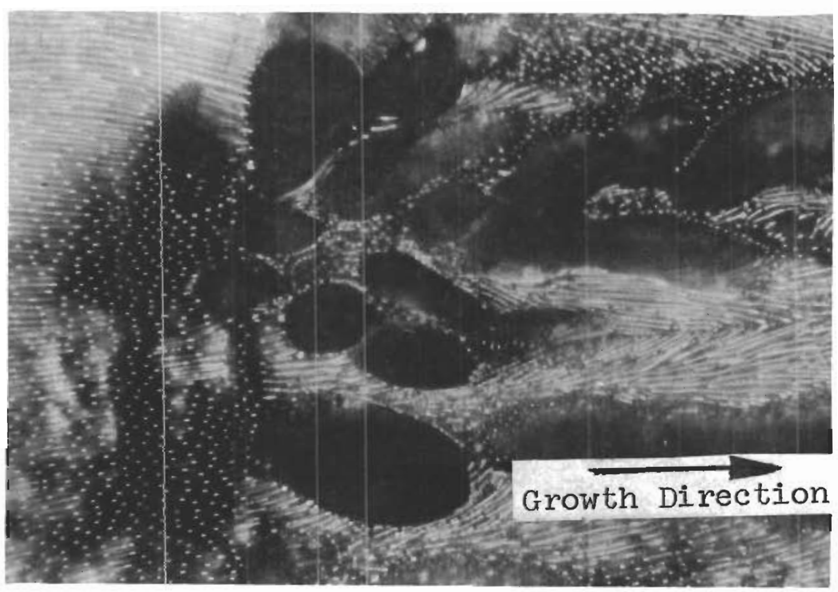

b) Longitudinal Section, Dark Field, 600X

Figure 6. Composite Areas Containing Primary Oxide and Eutectic Structure in ZrO_2 - 10 mole % Y_2O_3 - 5 weight % W.

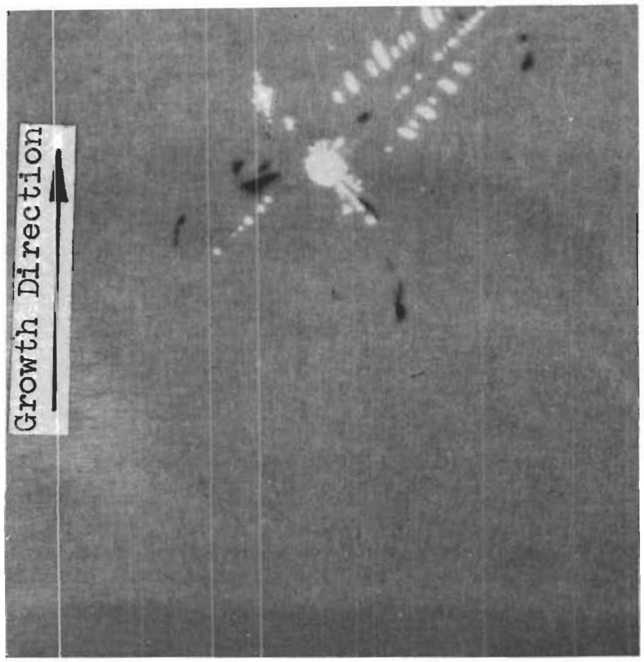

a) Bright Field, 600X

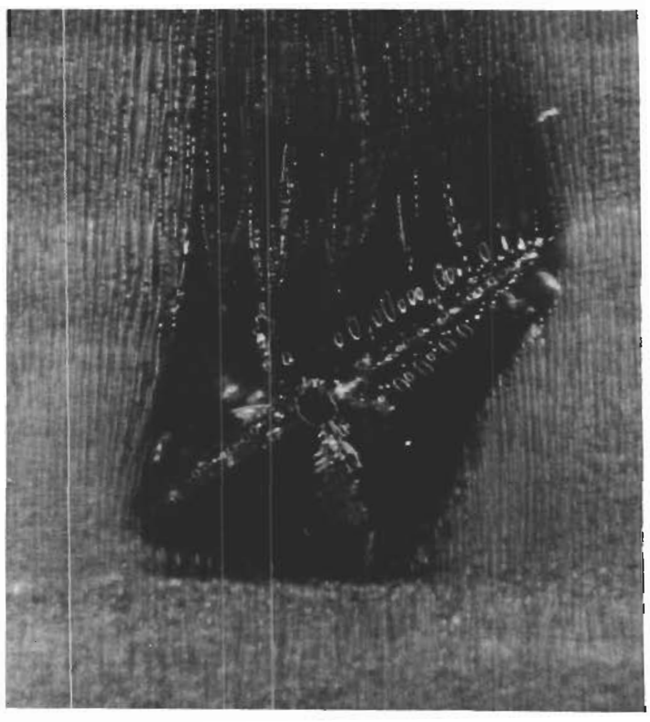

b) Dark Field, 600X

Figure 7. A Tungsten Dendrite Surrounded by an Oxide Halo and Eutectic Structure in ZrO_2 - 10 mole % Y_2O_3 - 17 weight % W.

remain the same as the initial starting mixture. In addition to other parameters, Table 1 tabulates the composition in the eutectic structure in weight percent W calculated from fiber sizes and density counts taken from SEM micrographs of well grown areas of ZrO_2-10 mole percent Y_2O_3-W samples. To convert the volume percent W to weight percent, the theoretical density of tungsten, 19.3 gm/cm^3, was used for the fibers. The density of the stabilized ZrO_2 (6.1 gm/cm^3) was determined by x-ray methods and checked by direct measurement on a sample not containing any W. A typical density for the solidified portion of the composites was 6.3 gm/cm^3. An error analysis on the composition calculations indicated the accuracy of these calculations to be about $\pm$ 2 weight percent W.

Solidification of ZrO_2-10 mole percent Y_2O_3-W samples in a H_2 only atmosphere differed from the solidification in the 90% N_2 - 10% H_2 atmosphere. In the H_2 atmosphere pellets containing as low as 8% W produced W dendrites in the fiber area. A composition of ZrO_2-10 mole percent Y_2O_3-6.5 weight percent W produced the best results in the H_2 atmosphere. This resulted in only a small amount of primary oxide at the top of the pellet and no W dendrites. If 6% W was used, this primary oxide area was slightly larger.

Influence of Growth Rate

The effect of growth rate on the fiber size and density of a series of ZrO_2-10 mole percent Y_2O_3-W samples solidified in 90% N_2 - 10% H_2 atmosphere is shown in Table 1. Micrographs of two samples grown under the same conditions except for about a tenfold change in growth rate are shown in Figure 8. Figure 9 illustrates the effect of growth rate on the fiber

Table 1. Fiber Size, Fiber Density, Composition, and Growth Rate Data for Some ZrO_2-10 Mole Percent Y_2O_3-W Samples

Sample Number	Weight % W Added	Growth Rate in cm/hr	Fiber Diameter Microns	Fiber Density x 10^{-6} Fibers/cm^2	Volume % Fibers	Calculated Eutectic Weight % W
6-80	15	0.34	0.95	--	---	---
18-57	15	1.06	0.74	7.6	3.3	9.8
6-67	15	1.75	0.52	12.5	2.6	7.9
18-67	16	1.94	0.47	14.5	2.5	7.6
18-59	17	2.17	0.45	12.3	1.9	5.9
6-82	15	2.59	0.40	10.8	1.3	4.2
18-70	16	3.62	0.31	31.8	2.4	7.3
18-74	16	5.87	0.22	48.7	1.9	5.8

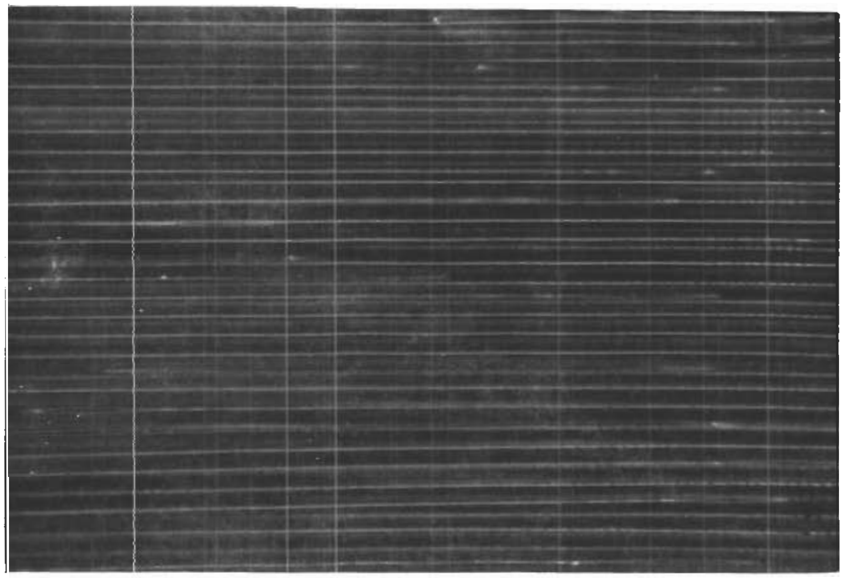

a) Growth Rate 0.51 cm/hr, Dark Field, 600X

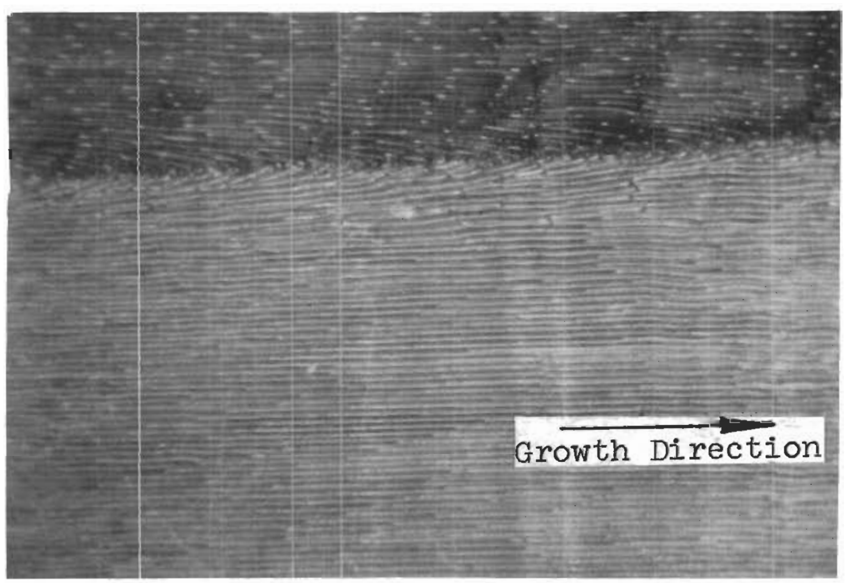

b) Growth Rate 5.9 cm/hr, Dark Field, 600X

Figure 8. The Effect of Growth Rate on Fiber Density in ZrO_2 - 10 mole % Y_2O_3 - 16 weight % W.

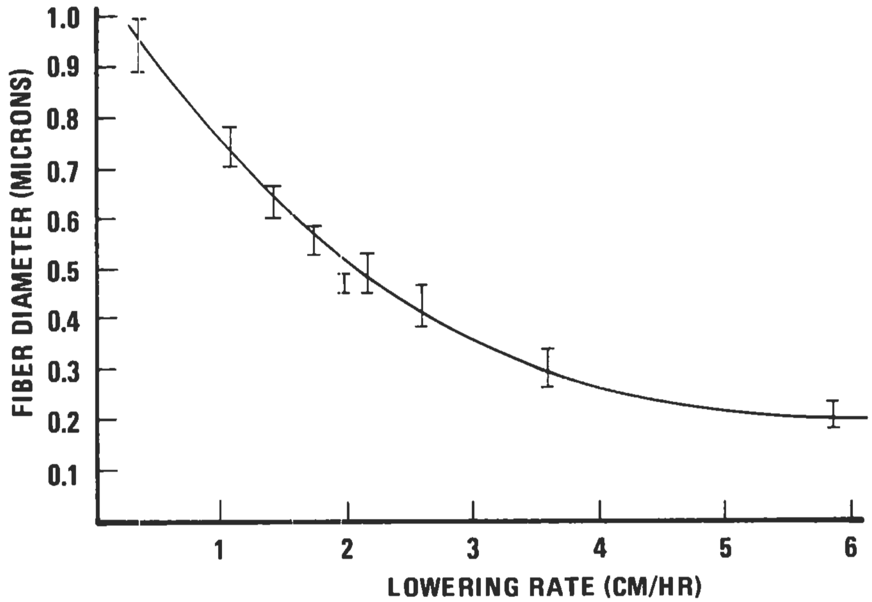

Figure 9. The Effect of Varying Growth Rate on the W Fiber Diameter in Y_2O_3 Stabilized ZrO_2 - W Samples.

diameter. Another effect noted especially at the higher growth rates was a tendency for small voids to be left in the solidified area of the pellet. The void that is normally at the top of the pellet would sometimes not travel completely to the top with growth rates above about five cm/hr.

General Description of the Composite

This section describes the various aspects of the Y_2O_3 stabilized ZrO_2-W composites not covered by the previous sections. The gross features of the solidified pellet are described along with details on grains or colonies, banding, and solidification of platelets.

Figure 10 shows a typical unidirectionally solidified pellet which has been cut in half, mounted in quickmount, and polished. The black area is the material that has been molten and unidirectionally solidified. Around the solidified material is the thin unmelted skin. The skin thickness varied from about 2 to 0.5 millimeters near the base where it almost melted through. The large void at the top of the pellet was due to the difference in the density of the solidified and unmelted material. Smaller voids were trapped at the bottom of the solidified zone due to the molten material being more viscous because of a lower temperature near the base of the pellet. The higher viscosity prevented these voids from raising to the top of the pellet. The light lines in the black solidified material are cracks in the pellet.

Figure 11 shows an area of uniform fiber growth. This polished section was cut normal to the lowering direction so it shows the end view of the fibers. Notice the hexagonal array in which the fibers solidify.

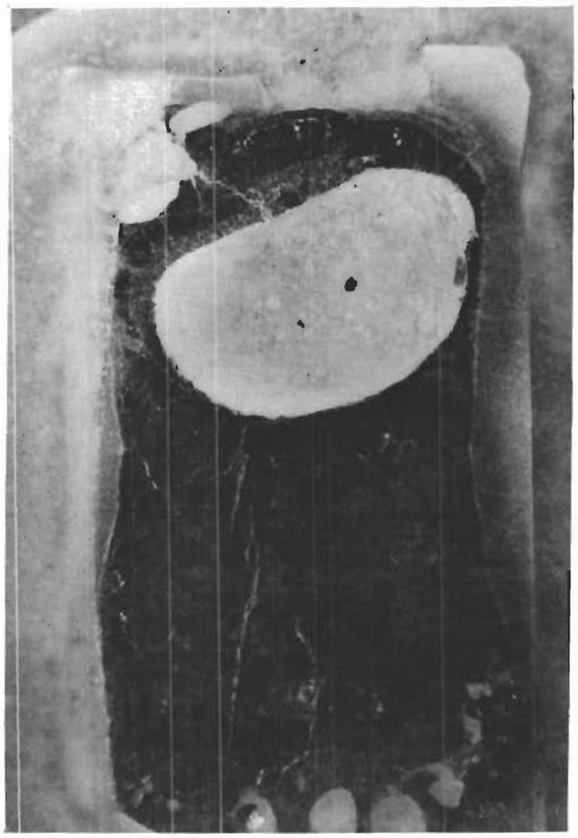

Figure 10. Typical Longitudinal Section of a ZrO_2 - Y_2O_3 - W Pellet Showing the Voids, Unmelted Skin and the Black Solidified Area. 5X

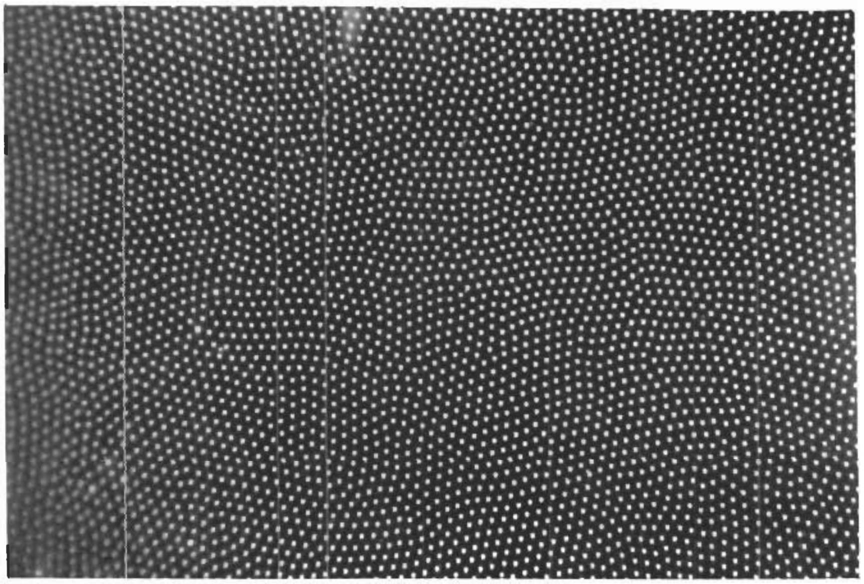

Figure 11. Typical Area of Uniform Fiber Growth in ZrO_2 - Y_2O - W Composites. Growth Direction Is Normal to Polished Plane. Dark Field, 600X

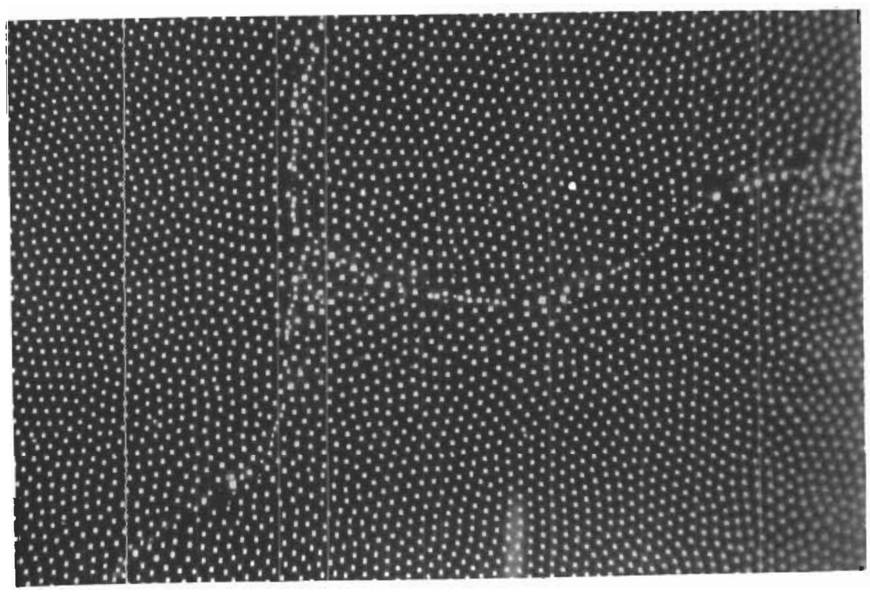

Figure 12. The Intersection of Three Grain Boundaries or Possibly Colony Walls in ZrO_2 - Y_2O_3 - W. Growth Direction is Normal to Polished Plane. Dark Field, 600X

Figure 8 from the previous section shows samples which were cut parallel to the lowering direction so the fibers can be seen lengthwise.

The boundaries between three grains or possibly colonies are seen in Figure 12. These boundaries can be seen lengthwise in Figures 8 and 13. To determine if these boundaries are grain boundaries or colony walls would require x-ray studies on the crystallographic orientation of the oxide matrix in the various grains or colonies. If they are grain boundaries, there would be a change in crystal orientation across the boundary unless by chance the grains had exactly the same orientation. If they are colony walls or cell boundaries (which are subcells of a grain), there would be no change in crystal orientation across the boundary since all the matrix in one grain is a single crystal. Since it has not been determined (because of the experimental difficulties of obtaining a very small x-ray beam) if they are grain boundaries or cell boundaries, they will be referred to as just "boundaries."

At these boundaries the fibers curve into the boundary. Since the fibers always solidify perpendicular to the liquid solid interface, the fiber curvature indicates there was a depression in the generally flat liquid-solid interface at the boundary. Figure 13 also shows how the boundary will cross a horizontal band of pure oxide. Notice how the fibers spread in a fan shape away from the boundary just above the oxide band. This indicated that the solidification of the fibers was nucleated at the boundary and that there might have been a concentration of impurities at the boundary which caused a localized lowering of the solidification temperature. This caused the slight depression in the flat liquid-solid

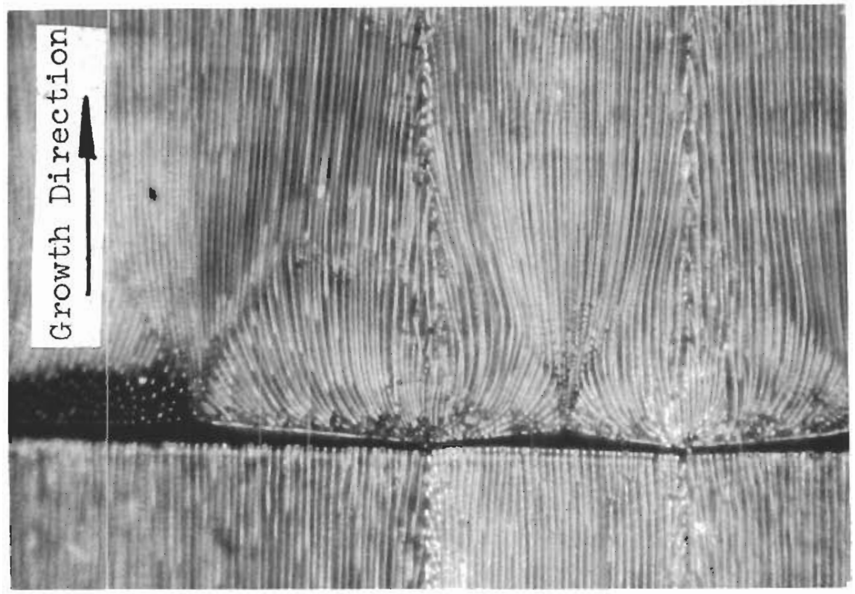

Figure 13. An Oxide Band in which the W Fibers Renucleate in a Fan Shape. Dark Field, 600X

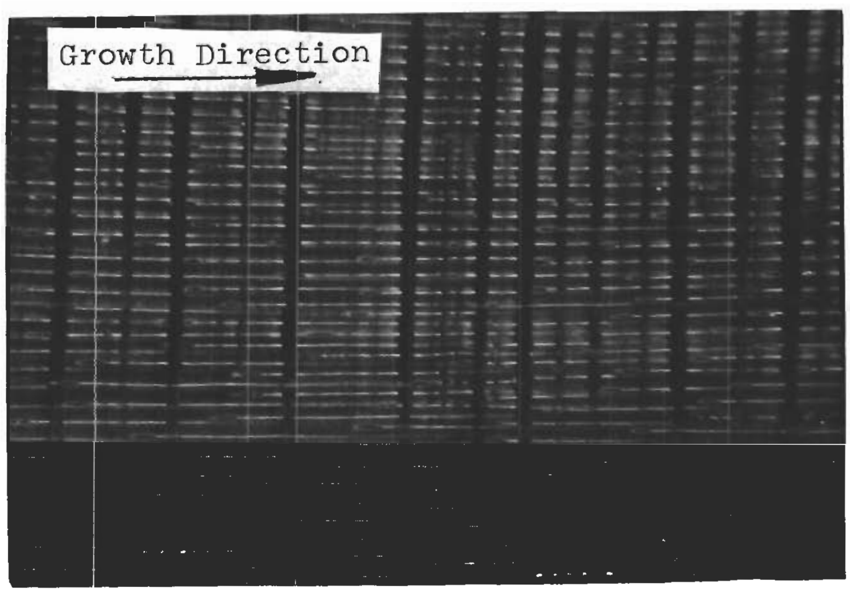

Figure 14. Oxide Bands in which the W Fibers Renucleate Just Above the Preceding Fibers. Notice the Few Fibers That Cross the Band. Dark Field, 600X

interface. Also, the impurities probably acted a site for nucleation of the solidification of the W fibers.

Horizontal bands interrupting the uniform solidification of fibers was a problem in many samples. Two types of bands were seen in the pellets. Figure 13 shows an oxide band in which the fibers renucleate in a fan shape. Usually such oxide bands are wider than those in Figure 13. Figure 14 shows another type of banding in which the fibers renucleate immediately above the terminated fiber. In Figure 14 a few fibers can be seen crossing the oxide band without interruption. The percentage of fibers that crossed this type of banding was very small.

In an attempt to find the cause of banding in the oxide-metal composites, power fluctuations were intentionally introduced during the solidification of a pellet. The plate current was lowered about 0.2 amp for about four seconds and then turned back up to the normal setting. This was done every ten minutes during the lowering of a sample. Figure 15 shows the type of banding produced by this major fluctuation in power. Notice the large W droplets that can be seen in the bright field view and in the dark field view the slight fan shaped form caused by the nucleation of several fibers from a single point. The W drops in the power fluctuation band distinguish this type of band from the type seen in Figures 13 and 14. Even larger bands of the type in Figure 13 never had W droplets in the oxide band. Power fluctuation type bands were occasionally seen in pellets solidified without deliberatively introduced power fluctuation, but these growth discontinuities were less frequent than the other type of bands. No definite cause could be established for the other types of bands.

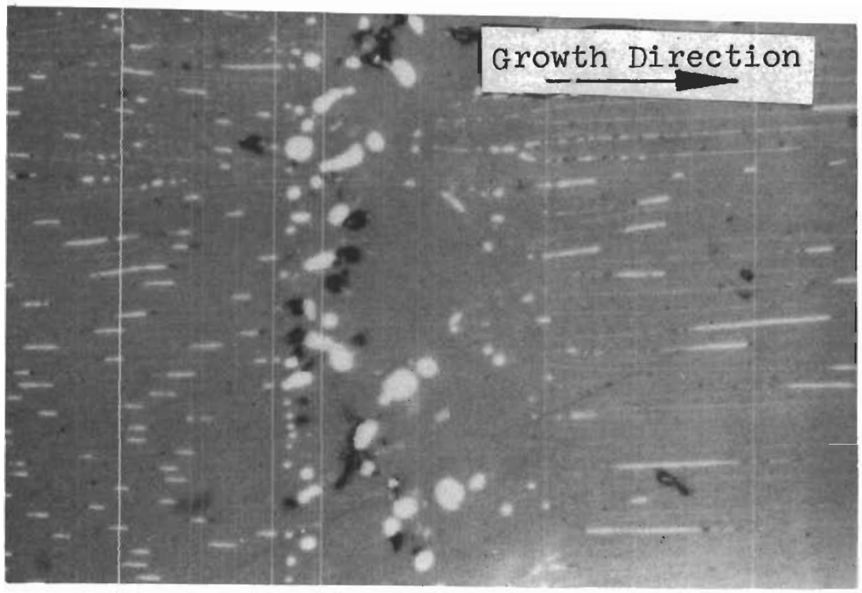

a) Bright Field, 600X

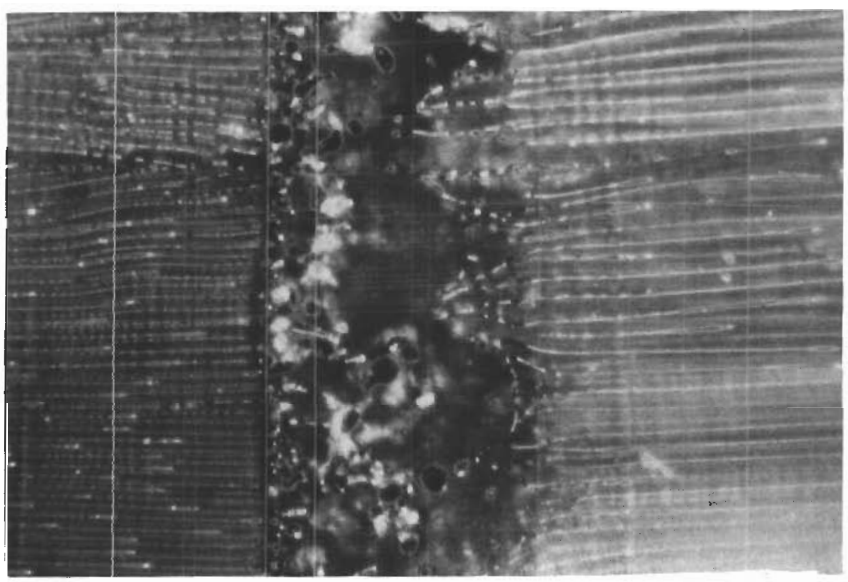

b) Dark Field, 600X

Figure 15. Wide Growth Discontinuity or Band Artificially Produced by a Power Fluctuation.

They may be a result of variations in the lowering rate or variations in the composition of the molten material or other unknown reasons.

Figure 16 shows another solidification morphology that was seen in isolated areas of a few samples. In this type of solidification the oxide matrix was always clear and transparent instead of dark and almost opaque. The W solidified in platelets with no apparent orientation. The transparent matrix made possible the viewing of these platelets relatively deep below the polished surface. This transparent matrix also caused many of the platelets to be out of focus in Figure 16.

A sample which was etched in boiling phosphoric acid for 14 hours is shown in Figure 17. The acid selectively etches back the matrix leaving the unetched W fibers protruding from the remaining matrix. SEM photos such as Figure 17 were used to determine fiber diameters. Similar SEM photos at about 2000X were used to count fiber densities.

Figure 18 shows a ZrO_2-Y_2O_3-W sample which had the W removed by etching with a solution of 100 ml distilled water; 7.5 grams, $K_3Fe(CN)_6$; and 2.5 grams, Na(OH). Notice the hexagonal shape of these holes indicating the fibers are probably not circular but hexagonal in cross section.

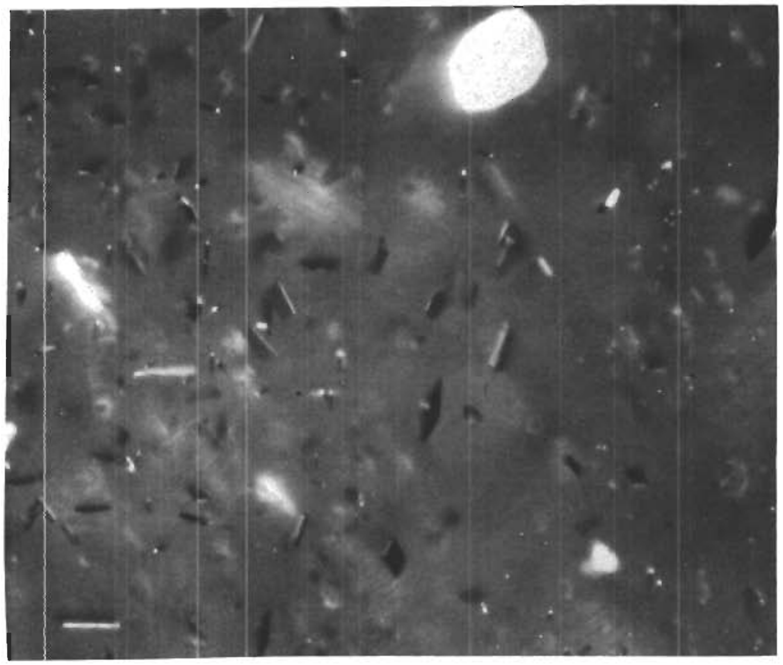

Figure 16. An Area of W Platelets in $ZrO_2 - Y_2O_3 -$ W. The Oxide in this Area Is Transparent Allowing Platelets Deeper than Usual To Be Seen in the Sample. Dark Field, 600X

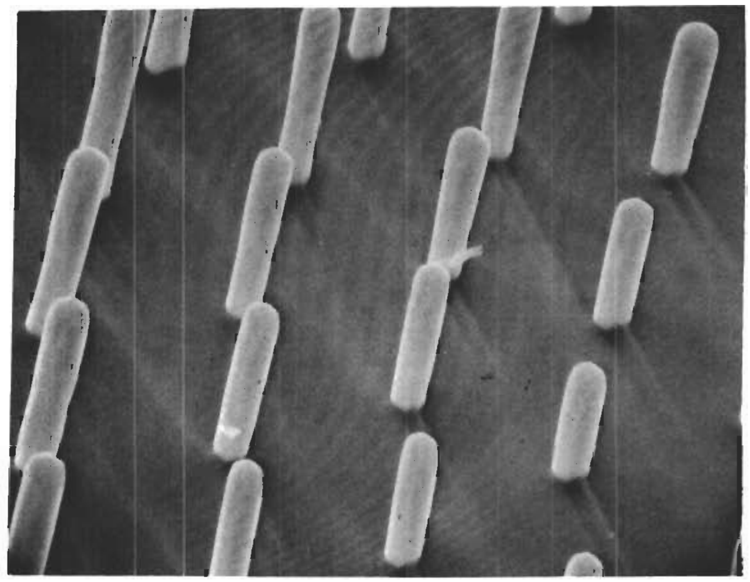

Figure 17. The W Fibers Protruding from the ZrO_2 - Y_2O_3 Matrix that Has Been Selectively Etched. SEM Photo at 6950X

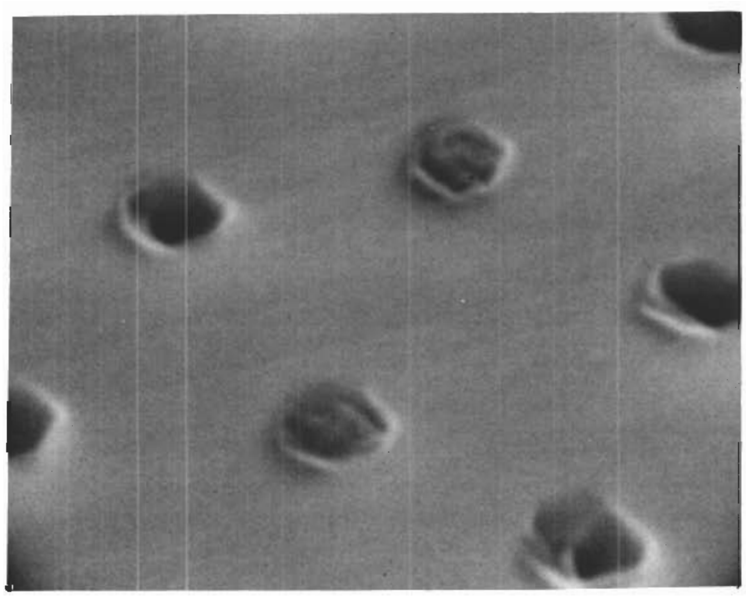

Figure 18. The ZrO_2 - Y_2O_3 Matrix with Holes Produced by Selectively Etching Away the W Fibers. SEM Photo at 24,700X

CHAPTER VI

DISCUSSION OF RESULTS

This chapter is a discussion and interpretation of the results presented in Chapter V. The chapter is divided into two sections. The first section concerns the establishment and control of a stable internal molten zone in Y_2O_3 stabilized ZrO_2-W pellets. The second section discusses the results in view of the solidification process and microstructure obtained in the composite. The coupled zone theory is used to explain some of the solidification phenomena.

Control of the Internal Molten Zone

In order to solidify oxide-metal composites by the internal molten zone technique a well controlled molten zone must be established within the sample pellet. Parameters that affect the formation of an internal molten zone include the electrical and thermal conductivity, density, melting point, composition, and temperature of the oxide-metal sample pellet. The induction heating frequency, input power, load coil geometry, and atmosphere are parameters concerning the induction heating process that also affect the establishment and control of the internal molten zone. The major difficulty that must be overcome by the understanding and control of these parameters was the initial establishment of a molten interior and the containment of the molten material by the thin unmelted sample skin. Since the heat was generated within the sample pellet by induction heating the surrounding atmosphere is cooler than the pellet itself. At the very high temperatures necessary to melt the refractory oxide-metal pellets, the heat loss from the sample skin by radiation loss was very high. This heat loss by radiation was great enough to establish a very steep thermal gradient on the outer few millimeters of the pellet. If the input power and heat loss were precisely balanced, the internal molten zone could be contained by a solid outer skin maintained at a lower temperature.

The initial formation of a stable molten zone is the most critical aspect of the internal molten zone technique. In order to establish the molten zone in a stabilized ZrO_2-W pellet using a 10 KVA output Lepel generator, the pellet must be preheated to increase the conductivity of the oxide. At the temperature of approximately $1600^{\circ}C$, the oxides' electrical conductivity was high enough to allow eddy currents to cause induction heating and the subsequent melting of the oxide. The frequency of the induction heating greatly affected the power necessary to establish these eddy currents. The higher the frequency the less power was needed to establish the eddy current heating within the oxide-metal pellet. At frequencies of 16 and 7.6 megahertz the pellet could be melted easily after preheating to $1600^{\circ}C$. At 3.6 megahertz more power was necessary to establish eddy current heating and the operator had to be skilled and accustomed to the method. After the molybdenum preheat tube was lowered, the power had to be quickly increased to a maximum before the pellet cooled too much. After the eddy currents were established in the pellet and the pellet was heating rapidly, the power had to be decreased at precisely the correct moment to prevent overheating and the molten interior from melting through the solid skin. If the operator did not have experience in this procedure, the pellet would usually not be melted or the molten interior would melt through the skin and be spilled. The only way of acquiring this experience was through many attempts and failures.

The frequency of the induction heating also affects the control of the molten zone. Equation 11 in Chapter II shows that the frequency has an inverse effect on the skin depth in induction heating. This skin depth was a measure of depth within a cylindrical work piece that an equivalent current would flow to produce the same current density as in the actual work piece. The skin depth is an indication of where most of the induction heating takes place in the cylindrical work piece. At very high frequencies the skin depth was very small so the heating was taking place very near the surface of a pellet. This would cause a thinner solid skin around the molten interior of a sample pellet than if a lower frequency were used. When using induction heating frequencies of 16 and 7.6 megahertz, the solid skin thickness was much thinner than at 3.6 megahertz. This very thin skin made control of the molten zone much more difficult in regard to preventing the molten interior from melting through the solid skin. The thicker solid skin was a major consideration in the use of the lower 3.6 megahertz frequency.

Lower frequencies than 3.6 megahertz should produce even thicker skins which would make control of the molten zone less difficult. At lower frequencies, however, the initial establishment of eddy currents would require higher preheat temperaturea and higher powers and result in increased difficulty in preventing the spilling of molten material. With the 3.6 megahertz frequency a stable molten zone could be established and controlled even though there was some difficulty. Consequently, most of the successful experiments used 3.6 megahertz.

The amount of Y_2O_3 stabilizer in the oxide mixture affected the formation of a molten zone. At Y_2O_3 contents above 10 mole percent there was much difficulty in establishing the eddy currents necessary for induction heating. Pellets containing as high as 20 mole percent Y_2O_3 could not be melted with 3.6 megahertz after preheating to approximately 1900°C. Apparently the conductivity of the oxide mixture decreased with increasing Y_2O_3 content and above 10 mole percent the conductivity was too low at 1600°C for sufficient eddy currents to be established. This effect might be avoided by very high preheat temperatures or possibly the addition of a third oxide which would raise the conductivity of the mixture.

The control of the molten zone, once it was established, was the next step. The molten zone could easily melt through the thin solid skin of the pellet if the temperature was too high. If the temperature was too low voids about one to three millimeters in diameter were left throughout the entire unidirectionally solidified material. There was no way to accurately monitor the temperature of the skin of the pellet due to the vapor deposits continuously forming on the silica tube that prevented accurate or reproducible measurements with the optical pyrometer. The only control of the pellet temperature was through careful control of the power settings on the Lepel induction generator. The range of power settings allowing good solidification was very narrow being about .02 amp on the plate current for any fixed composition and growth atmosphere. The correct power setting varied with any change in composition from pellet to pellet and any change in atmosphere.

Changes in pellet composition affected the liquidus temperature of the material. Assuming everything else constant, if the sample compositions were changed successively toward the actual eutectic composition (or toward the boundary curve between the two primary phases if you consider the actual three component phase diagram), the liquidus temperature would be lower for each successive composition. This liquidus temperature would be the temperature at the interface between the molten interior and the unmelted skin if equilibrium was established at that point. The induction heating power needed to maintain a solid skin of equal thickness would then be decreasing with each change in composition. This ideal situation was complicated by slight changes in the electrical and thermal conductivity with changes in composition. Changes in the electrical conductivity are are reflected in the load the Lepel generator sees and thus the heating efficiency at any given power level. Changes in the thermal conductivity affect the temperature gradient across the solid skin and thus affect the thickness of the skin. Both of these effects are probably very small in comparison to other variables, but they would prevent any accurate prediction of the power setting necessary to achieve the temperature needed for good unidirectional solidification. The power setting needed for each change in pellet composition was established by a trial and error process that usually required three or four experiments before the correct setting was found.

Changes in the atmosphere also affected the necessary power settings.

Atmospheres used were N_2, H_2, or mixtures of these gases. An atmosphere of H_2 had a much greater cooling effect on the pellet surface than a N_2 atmosphere. Differences of approximately 200°C on the pellet surface were measured in H_2 or N_2 atmospheres with all other variables held constant.

It is also possible that the atmosphere affected the composition of the oxide in the pellet. In non-stoichiometric oxides the oxygen partial pressure affects the equilibrium metal to oxygen ratio in the oxide. The reaction rate of this atmosphere-oxide reaction may be very fast at the high temperatures of the molten oxides so long times to achieve equilibrium may not be necessary to complete reactions. Carniglia et al.[48] reported that ZrO_2 is non-stoichiometric at high temperatures. Chapman et al.[49] have investigated the equilibrium between molten non-stoichiometric $UO_{2\pm x}$ and atmospheres of various oxygen pressures. The experimental method and equipment were similar to the internal molten zone technique used for unidirectional solidification of composites. Changes in the atmosphere around the UO_2 similar to changes in this investigation produced significant changes in the oxygen to uranium ratio. Similar effects might occur in the molten ZrO_2. These changes might affect the liquidus temperature and power requirements in the same manner as changes in the pellet composition. Such effects on power requirements are probably negligible but they could affect the tungsten solubility in the molten oxide. This is discussed in the following section on composite microstructure.

The solidification rate or lowering rate did not have a great effect on the control of the molten zone. The only effect noticed (except on actual fiber density and size) was that at lowering rates above six cm/hr small voids formed that were similar to those seen when the power was too low. The difference in density of the molten and solidified material produced these voids and at very high growth rates the voids did not have time to flow to the top of the pellet to produce the large void usually occurring above the solidified material.

The actual size of the internal molten zone could have an effect on the stability of the zone. Observations of the temperature gradient along the length of ZrO_2-Y_2O_3-W pellets showed a relatively narrow (about one centimeter), very high temperature zone with a sharp thermal gradient on the sides of the zone. This indicated there was a relatively small internal molten zone. During composite growth solid material melted from the top of the zone and the liquid material solidified at the base as the pellet was lowered. In other oxide-metal systems such as UO_2-W almost the whole length of the pellet had the same high temperature indicating that there was a molten pool almost the entire length of the pellet at the beginning of unidirectional solidification.[13] With a small molten zone as in the ZrO_2-Y_2O_3-W system, fluctuations in the induction heating power would have a greater effect since it was concentrated in a smaller volume. Compositional variations in the oxide-metal mixture along the length of the pellet would also have a greater effect on a small zone because of the constant melting and solidification of material as the pellet was lowered. For large molten zones any initial composition variations would be eliminated by the mixing of all the material in the long molten zone before the solidification began. It would be desirable to obtain a larger molten zone in ZrO_2-Y_2O_3-W but a simple increase in induction heating power caused the solid skin to melt. A change in the induction heating coil geometry which distributed the electromagnetic field over a wider section of the pellet might increase the size of the internal molten zone.

Composite Microstructure

The composite microstructure formed during the unidirectional solidification of Y_2O_3 stabilized ZrO_2-W consisted of small parallel W fibers uniformly aligned in the oxide matrix. The W fibers were generally continuous but bands perpendicular to the fibers often interrupted the fiber growth. The size and density of the fibers varied with the solidification rate but values of 0.4 micron in diameter and 11×10^6 fibers per square centimeter were typical. The composition of the pellet had a major effect on the microstructure with the amount of W having a greater effect than variations in Y_2O_3 stabilizer content.

The microstructure varied somewhat across the pellet. This is shown schematically in Figure 19. Throughout the central core (approximately 50% of the volume of the pellet) the fibers were parallel to the lowering direction. On the outer portions of the solidified zone the fibers were parallel to each other but were curved upward following the temperature gradient toward the hotter melt. Adjacent to the unmelted skin the fibers nucleated and solidified perpendicular to the pellet walls. These fibers curved upward as they solidified toward the center of the pellet so in the central core all the fibers were parallel to the pellet walls or lowering direction. If a line were drawn across the pellet so that it was perpendicular to the fibers, this line would lie on the plane of the liquid-solid

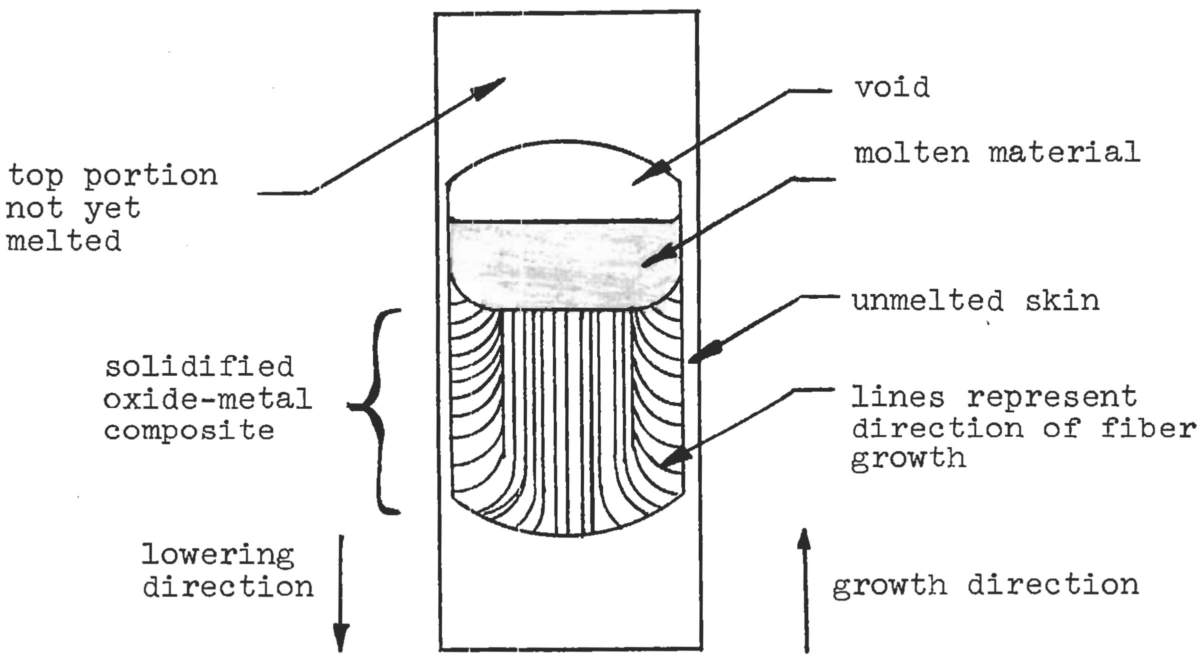

Figure 19. Schematic Diagram of a Pellet During Unidirectional Solidification

interface at the moment of solidification of those fibers. The curvature of the liquid-solid interface near the pellet walls was due to the heat flow out of the pellet through the walls. At the center of the pellet the heat flow followed the direction of the fibers toward the base of the pellet. This heat flow toward the base of the pellet was the basis for unidirectional solidification as opposed to a usual solidification process. The flat liquid-solid interface was necessary to produce parallel aligned fiber growth.

The flat interface was interrupted on a very small scale at the grain boundaries or colony walls mentioned in Chapter V and shown in Figures 8b and 13. Figure 20 shows the shape of the interface at these boundaries. To produce the curvature of the fibers at the boundary, the interface must have a slight depression. If these boundaries are grain boundaries, the depression may be due to a higher concentration of impurities at the boundary. The impurities would lower the liquidus temperature in a localized region and result in the material at the grain boundary to be solidified slightly later than the neighboring material in the center of a grain. This lag in the solidification at the grain boundary resulted in the depression in the liquid-solid interface.

If the boundaries are cell boundaries or colony walls, they are caused by a "constitutional undercooling" as explained by Tiller.[33] The cells or colonies seen in metal-metal composites appear very different from the areas outlined by the boundaries in oxide-metal composites. A different distinction between grains and colonies can only be made by a detailed x-ray analysis, but it appeares that the areas are probably grains and not colonies.

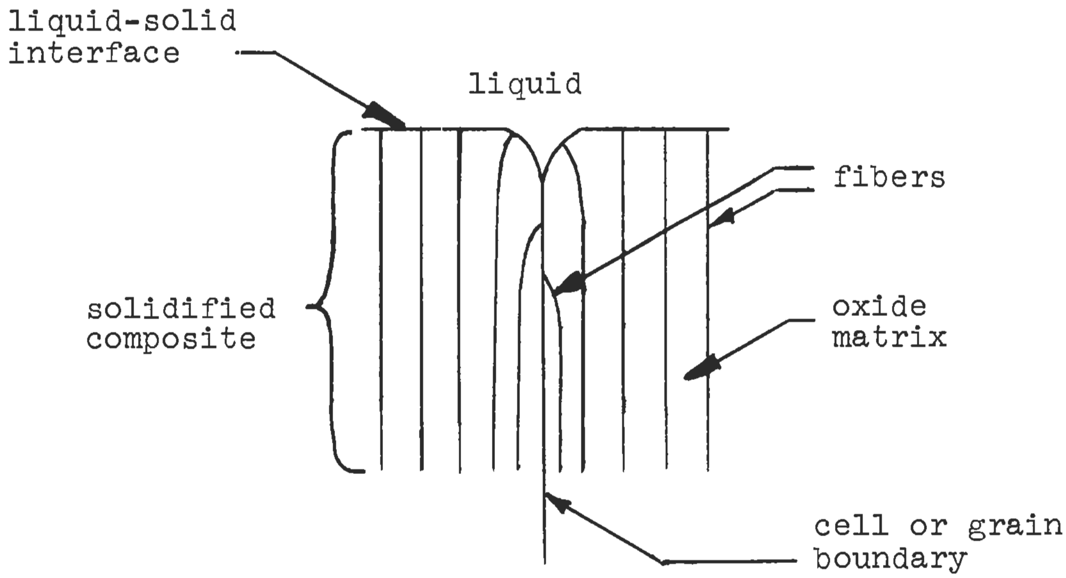

Figure 20. Schematic Diagram of the Depression in the Usually Flat Liquid-Solid Interface at a Cell or Grain Boundary.

Figure 13 provides more evidence for grains as opposed to colonies. A boundary is seen crossing a horizontal oxide band. The solidification of the oxide band would have interrupted the temperature distributions necessary for constitutional undercooling, which is necessary to form colonies. It is unlikely that colony walls would be reestablished directly over the previous colony wall. If the boundary is a grain boundary, the boundary would cross the oxide band without interruption as it does. Since the oxide within either grain is continuous across the band in Figure 13, the crystal orientation of the oxide matrix does not change across the horizontal band. Since it is the oxide matrix which determines the eutectic grains, the material above and below the horizontal band must be in the same eutectic grain. A grain boundary would then be able to cross an oxide band which interrupts the metal fiber solidification.

There are three types of horizontal bands that interrupt the fiber solidification. The first type of band is shown in Figure 13 and always has the W fibers renucleating above the oxide band and spreading in a fan shape in the two dimensional photograph. If observed in three dimensions, the fan would usually appear as a triangular prism with its apex pointed down and centered on a grain boundary. The prism is a group of fibers that has been nucleated at the grain boundary. Impurities in the molten material or the actual grain boundary would be acting as the nucleation site. Some "fans" in this type of banding do not lie on a grain boundary but in the center of the grain. These "fans" would appear as cones of fibers in three dimensions with the nucleation site as a point on the liquid-solid interface.

The exact cause of the horizontal oxide bands of the type in Figure 13 is not known exactly, but the coupled zone theory offers a possible explanation. If the liquid composition and amount of undercooling at the liquid-solid interface lie within the coupled zone but very near to the oxide rich boundary of the zone, a eutectic structure would be solidified. A slight change in the liquid composition at the interface which enriched the liquid in the oxide would move the growth conditions out of the coupled zone. The oxide phase would advance ahead of the W fiber phase and spread the short distance across the top of the W fibers. The W in the liquid would be prevented from solidifying on the fibers by this oxide covering. The composition of the liquid would be shifted back toward the coupled zone by the solidification of the oxide band. When the liquid composition had shifted sufficiently, the W phase must nucleate above the oxide band. The W phase always nucleated as fibers and immediately solidified in a coupled manner in this type of banding. This indicated that the shift in liquid composition did not cross the coupled zone to the W rich side before the nucleation of the W phase.

The shift out of the coupled zone which started the oxide band could be caused by a slight variation in the undercooling instead of change in composition. The coupled zone is usually skewed toward the component with the higher melting point, in this case the W. A slight increase in the undercooling would shift the growth conditions out of the coupled zone to the oxide rich side without changing the actual liquid composition. The oxide band would be solidified just as explained above and a localized shift in the liquid composition at the interface would move the growth conditions back into the coupled zone. A decrease in the amount of undercooling might accompany this composition shift. Mixing with the bulk of the liquid would shift the local liquid composition at the interface back to the composition that was being solidified before the oxide band. All growth conditions would be the same as before the oxide band was solidified.

To prevent this type of banding the growth conditions must be very stable and lie within the coupled zone. If the growth conditions lie in the center of a wide coupled zone, larger fluctuations in local composition and undercooling at the interface can be tolerated by the system and still produce coupled growth.

The second type of oxide banding is shown in Figure 14. In this type of banding the W fibers renucleate just above the previous fiber. These oxide bands were always very thin whereas in the "fan" type of banding in Figure 13 the oxide band varied in width and was often much wider than shown in Figure 13. A few fibers cross the oxide bands as shown in Figure 14 and, although this behavior was rare, it definitely occurred. A good explanation of this type of banding has not been developed. It might be related to sudden sharp variations in the lowering rate caused by sticking of the hydraulic cylinder which controls the lowering of the pellet.

The third type of banding shown in Figure 15 was caused by fluctuations in the power. This would cause sudden changes in the temperature of the liquid and might cause sudden rapid solidification or remelting of the material. This type of banding is easily recognized by the large W drops in the band. These power fluctuation bands were occasionally seen in samples but were not as common as the "fan" type of banding.

Solidification of the primary oxide seen in Figure 6 and W dendrites in Figure 7 can be explained in terms of the coupled zone and nucleation factors. Primary oxide areas were always surrounded by the eutectic structure with the oxide phase continuous from the primary oxide into the eutectic structure. Tungsten dendrites were always surrounded by an oxide halo which was continuous with the oxide phase in the adjacent eutectic structure. In Chapter II the solidification of metal α halos around metal β dendrites was explained. This explanation can be extended to the oxide-metal system by considering the ZrO_2-Y_2O_3 phase as the α phase and the W phase as the β phase. The properties of the metal α phase in Chapter II were a complex crystal structure that is difficult to nucleate but acts as a good nucleating agent and forms a halo around the β phase. The metal α properties then correspond to the properties of the ZrO_2-Y_2O_3 phase. The metal β phase in Chapter II had the properties of a simple crystal structure which is easy to nucleate but acts as a poor nucleating agent and did not form halos around the α phase. These properties correspond to the W component. (For the detailed explanation of the solidification of oxide halos around the W dendrites, the reader should read the section in Chapter II and refer to Figure 3 with the substitution of ZrO_2-Y_2O_3 for the α phase and W for the β phase in mind.)

An explanation of the solidification of ZrO_2-Y_2O_3 primary oxide regions that are continuous with the oxide phase in the adjacent eutectic structure is simple in view of the properties mentioned above. If the liquid is rich in the oxide components and the coupled zone is skewed toward the W component which has a higher melting point, the oxide phase will solidify at a faster rate than the eutectic structure. Primary oxide regions would then solidify extending into the liquid above the normally flat liquid-solid interface. The liquid between these primary oxide regions and also above them would be depleted of the oxide components moving the liquid composition into the coupled region. The W phase is easy to nucleate on the solid primary oxide so the eutectic structure can begin solidifying without a large supersaturation of the liquid with W. The oxide phase solidifies in the eutectic structure continuous with the primary oxide.

If the W phase was difficult to nucleate the liquid would have to be highly supersaturated with W and the composition might lie on the W rich side of the coupled zone. If this were the case (which it is not) a W halo would solidify around the primary oxide.

The solidification of primary oxide in the upper portions of the pellet was common when the 90% N_2 - 10% H_2 atmosphere was used. Table 1 indicates that the initial W content in these pellets was considerably larger than the W content in the solidified composite. This behavior can be explained by vaporization of the W from the sample. In these experiments the silica tube slowly became coated with a vapor deposit. X-ray analysis of this deposit indicated it contained metallic W and WO_2 and WO_3. The W content in the liquid was being depleted by vaporization and by the time the upper portions of the pellet were being solidified the W content was too low. Primary oxide then solidified at the top portions of the pellet.

The formation of tungsten oxides could be due to the ZrO_2 going substoichiometric and giving off oxygen which reacted with the W. This substoichiometric oxide would be the explanation of the black color of the oxide phase. Pellets of ZrO_2-Y_2O_3 without W melted and solidified in air were not black but clear with a slight yellow tint.

Solidification of ZrO_2-Y_2O_3-W in a H_2 on atmosphere required a much lower W content and there was much less vapor deposition on the silica tube walls. The increased H_2 content in the atmosphere could have prevented the formation of tungsten oxides by reacting with the oxygen given off by the ZrO_2 or by reducing the tungsten oxides back to W. This would have acted to contain the W in the pellet since the major portion of the W vaporization occurred as the tungsten oxides.

The H_2 content in the atmosphere would affect the very low oxygen partial pressure in the system. In the $UO_{2\pm x}$-W system the oxygen partial pressure controls the stoichiometry of the oxide phase. This in turn controls the solubility of the W in the molten oxide and is a very important factor in composite growth.[13] This could also be very important in the ZrO_2-W system, although the non-stoichiometric field is not as wide as in $UO_{2\pm x}$, and might be related to the W content necessary to produce optimum growth in the various atmospheres. A detailed study in which the oxygen partial pressure was controlled and monitored would be of interest in the ZrO_2-Y_2O_3-W system.

CHAPTER VII

CONCLUSIONS

1. The internal molten zone technique can be used to melt and unidirectionally solidify ZrO_2-Y_2O_3-W pellets containing between 7.9 and 10 mole percent Y_2O_3.

2. The samples could be melted easily after preheating to about 1600°C with the higher induction heating frequencies of 7.6 and 16 megahertz, but control of the molten zone was very difficult.

3. Reducing the induction heating frequency to 3.6 megahertz provided adequate control of the internal molten zone in the Y_2O_3 stabilized ZrO_2-W samples.

4. The precise control of the input power was very critical to prevent the formation of voids in the solidified material or to prevent the molten material from melting through the unmelted pellet skin.

5. The composite microstructure consisted of a single oxide phase containing W fibers aligned parallel to the solidification direction.

6. The solidification rate controlled the W fiber size and density with faster rates producing smaller fibers with a higher fiber density.

7. Typical W fiber size and density values for a 2.6 centimeter per hour solidification rate were 0.4 micron diameter and 11 million fibers per square centimeter.

8. The amount of H_2 in the N_2-H_2 atmosphere affected the power setting and oxide-metal composition giving the best composite solidification.

9. The most uniform composite solidification occurred using ZrO_2 - 10 mole percent Y_2O_3 - 16 weight percent W in a N_2 - 10% H_2 atmosphere but areas of primary oxide at the top of the solidified zone limited the length of uniform composite structure.

10. In a H_2 atmosphere fairly uniform composite growth was obtained almost the entire length of the solidified zone using ZrO_2 - 10 mole percent Y_2O_3 - 6.5 weight percent W.

11. The solidification of primary oxide regions from oxide rich compositions and W dendrites with oxide halos from W rich compositions are explained using the coupled zone and nucleation theories.

12. Three types of horizontal bands interrupting the continuous fiber growth were observed and possible causes of two of these discontinuities are given.

APPENDIX A

CHEMICAL ANALYSIS OF ZIRCOA A-HC ZIRCONIUM DIOXIDE POWDER BY ZIRCORIUM CORPORATION OF AMERICA

Element	PPM	
	lot 6474	lot 7970
Al	70	40
B	0.2	1
Ca	100	50
Cd	0.2	0.2
Cr	10	10
Co	10	5
Cu	10	10
Fe	80	80
Hf	50	50
Pb	10	10
Mg	70	50
Mn	1	1
Ni	10	10
Si	200	400
Ti	30	10
Va	10	10
W	100	--
C	--	160
Cl	30	10
F	72	0.3
SO_4	60	90
LOI	380	54

Analytical method was emission spectroscopy.

APPENDIX B

CHEMICAL ANALYSIS OF YTTRIA POWDER BY KERR McGEE CHEMICAL CORPORATION OF AMERICA

Element	PPM	
	lot D0717	lot D0909
Al	8	8.8
Ca	7	11
Mg	0.5	0.5
Fe	ND	11
Si	17	330
Rare earth oxides		
Pr_6O_{11}	4	4
Nd_2O_3	1	1
Sm_2O_3	4	4
Eu_2O_3	6	6
Gd_2O_3	ND	22
Tb_4O_7	4	30
Dy_2O_3	21	20

Also analyzed for but not detected (ND) were the elements B, Be, Bi, Co, Cr, Ge, Mn, Mo, Ni, Pb, Sb, Sn, Ti, Tl, V, Zn, and Zr. All other rare earth oxides were also not detected.

The method of analysis for those rare earth oxides detected was cathodoluminescence. The method for all other rare earths and the elements was spectrographically.

APPENDIX C

CHEMICAL ANALYSIS OF TUNGSTEN POWDER BY FAIRMOUNT CHEMICAL CORPORATION

Element	PPM lot 6049
Al	1
Ca	1
Cr	4
Cu	1
Fe	6
K	25
Mg	2
Mn	1
Mo	10
Na	38
Ni	17
Si	2
Sn	1

Average particle size was reported as 2.13 microns

Wah Chang Huntsville in a separate analysis reported these results for the tungsten powders.

Supplier	Oxygen PPM	Carbon PPM
Fairmount	1576	20
Fisher	640	3

BIBLIOGRAPHY

1. L. M. Hogan, "The Solidification of Binary Eutectic Alloys," Journal of the Australian Institute of Metals, Vol. 6, No. 4, 1961, p 279.

2. E. Scheil, "Uber die eutektische Kristallisation," Zeitschrift Metallkde," Vol. 45, 1954, p 298.

3. H. W. Weart and D. J. Mack, "Eutectic Solidification Structures," Transactions of the Metallurgical Society of AIME, 1958, p 664.

4. A. Kofler, "Uber die Ausscheidungsanomalien in unterkuhlten binaren Schmelzen, insbesondere uber die sogenannte Hofbildung," Zeitschrift Metallkde, Vol. 40, 1950, p 221.

5. J. D. Hunt and K. A. Jackson, "Binary Eutectic Solidification," Transactions of the Metallurgical Society of AIME, Vol. 236, 1966, p 243.

6. F. S. Galasso, W. L. Darby, F. C. Douglas, and J. A. Batt, "Unidirectional Solidification of the $BaFe_{12}O_{19}$-$BaFe_2O_4$ Eutectic," Journal of the American Ceramic Society, Vol. 50, 1967, p 333.

7. C. O. Hulse and J. A. Batt, "Preparation and Properties of Directionally Solidified ZrO_2-Y_2O_3 Eutectic," National Materials Advisory Board Report NMAB, 308-I, Jan. 1973, p 129.

8. M. T. Johnson, "Controlled Eutectic Solidification in the Al_2O_3-$Y_3Al_5O_{12}$ System," Bachelor's thesis in the School of Ceramic Engineering, Georgia Institute of Technology, 1970.

9. M. C. Pao, "Unidirectional Solidification of UO_2-RO Type Refractory Oxides with the Emphasis in the System UO_2-MgO," Master's thesis in the School of Ceramic Engineering, Georgia Institute of Technology, 1973.

10. F. Schmid and D. Viechnicki, "Oriented Eutectic Microstructures in the System Al_2O_3-ZrO_2," Journal of Materials Science, 1970, p 470.

11. D. Viechnicki and F. Schmid, "Eutectic Solidification in the System Al_2O_3-$Y_3Al_5C_{12}$," Journal of Materials Science, 1969, p 84.

12. L. M. Hogan, R. W. Kraft, and F. D. Lemkey, "Eutectic Grains," Advances in Materials Research, Vol. 5, editor, H. Herman.

BIBLIOGRAPHY (Continued)

13. A. T. Chapman, "Melt-Grown Oxide-Metal Composites," Technical Reports 1-5, sponsored by ARPA, contract numbers DAAHOI-70-C-1157 and DAAHOI-71-C-1046, ARPA order number 1637, 1971-1973.

14. A. T. Chapman, G. W. Clark, and D. E. Hendrix, "UO_2-W Cermets Produced by Unidirectional Solidification," Journal of the American Ceramic Society, Vol. 53, 1970, p 60.

15. A. T. Chapman, R. J. Gerdes, J. C. Wilson, and G. W. Clark, "Unidirectional Solidification Behavior in Refractory Oxide Metal Systems," Journal of Crystal Growth, Vol. 13, 1972, p 765.

16. R. J. Gerdes, A. T. Chapman, and G. W. Clark, "Refractory Oxide-Metal Composites: Scanning Electron Microscopy and X-ray Diffraction of Uranium Dioxide-Tungsten," Science, Vol. 167, 1970, p 979.

17. N. E. Grynkewich, "Factors Determining the Unidirectional Solidification Behavior of the System UO_2-W," Master's thesis in the School of Ceramic Engineering, Georgia Institute of Technology, 1972.

18. M. D. Watson, "ZrO_2-W Cermets Produced by Uniderctional Solidification," Bachelor's thesis in the School of Ceramic Engineering, Georgia Institute of Technology, 1969.

19. M. D. Watson, D. N. Hill, and A. T. Chapman, "Solidification Behavior of Stabilized ZrO_2-W," Journal of the American Ceramic Society, Vol. 53, 1970, p 112.

20. M. D. Watson, T. A. Johnson, J. F. Benzel, and A. T. Chapman, "Unidirectional Solidification of Tungsten in Stabilized ZrO_2 and HfO_2," Proceedings of the Conference on In Situ Composites, Lakeville, Connecticut, September 5-8, 1972, p 157.

21. T. A. Johnson, "Unidirectional Solidification of Tungsten in Stabilized Hafnia," Master's thesis in the School of Ceramic Engineering, Georgia Institute of Technology, 1972.

22. T. A. Johnson and J. F. Benzel, "Unidirectional Solidification of Stabilized HfO_2-W," Journal of the American Ceramic Society, Vol. 56, 1973, p 234.

23. C. Jen, "Factors Determining the Unidirectional Solidification Behavior of the Systems UO_2-Ta, UO_2-Nb, and UO_2-Mo," Master's thesis in the School of Ceramic Engineering, Georgia Institute of Technology, 1972.

BIBLIOGRAPHY (Continued)

24. R. P. Nelson and J. J. Rasmussen, "Composite Solidification in the Systems: Cr_2O_3-Mo, Cr_2O_3-Re, Cr_2O_3-W, and MgO-W," Journal of the American Ceramic Society, Vol. 53, 1970, p 527.

25. J. Briggs, personal communication, 1972.

26. F. L. Brady, "The Structure of Eutectics," Journal of the Institute of Metals, Vol. 28, 1922, p 369.

27. L. M. Hogan, "The 'Coupled Region' Concept in Eutectic Solidification," Journal of the Australian Institute of Metals, Vol. 9, 1964, p 228.

28. V. de L. Davies, "Mechanisms of Crystallization in Binary Eutectic Systems," Journal of Metals, Vol. 93, 1964, p 10.

29. G. A. Chadwick, Metallography of Phase Transformations, Butterworths, London, 1972.

30. G. A. Chadwick, "Controlled Eutectic Growth" in The Solidification of Metals, Iron and Steel Inst. ISI Publication 110, 1968.

31. G. A. Chadwick, "Eutectic Alloy Solidification," in Progress in Materials Science, Vol. 12, 1968, B. Chalmers editor, Pergamon Press, Oxford.

32. J. D. Hunt and K. A. Jackson, "The Dendrite-Eutectic Transition," Transactions of the Metallurgical Society of AIME, Vol. 239, 1967, p 864.

33. W. A. Tiller, "Polyphase Solidification," Liquid Metals and Solidification, ASM, p 276, Cleveland, 1958.

34. H. E. Cline, "Theory of the Lamellar Dendritic Transition in Eutectic Alloys," Transactions of the Metallurgical Society of AIME, Vol. 242, 1968, p 1613.

35. K. G. Davis and L. M. Hogan, "The Dendrite-Eutectic Transition in Tin-Lead Alloys Solidified with Low Temperature Gradients," Journal of the Australian Institute of Metals, Vol. 15, 1970, p 29.

36. A. Jackson, "The Dendrite-Eutectic Transition in Sn-Pb Alloys," Transactions of the Metallurgical Society of AIME, Vol. 242, 1968, p 1275.

37. L. M. Hogan, "Solidification of the Aluminum $CuAl_2$ Eutectic: The Influence of the Primary Phases," Journal of the Australian Institute of Metals, Vol. 7, 1962, p 188.

BIBLIOGRAPHY (Concluded)

38. B. E. Sundquist, R. Bruscato, and L. F. Mondolfo, "The Structure of Eutectics," Journal of the Institute of Metals, Vol. 91, 1962, p 204.

39. B. E. Sundquist and L. F. Mondolfo, "Heterogeneous Nucleation in the Liquid-to-Solid Transformation in Alloys," Transactions of the Metallurgical Society of AIME, Vol. 221, 1961, p 157.

40. M. Perez and R. Collongues, "Sur Le Chauffage et La Fusion Sans Creuset Par Induction Haute Frequency De Quelques Oxydes Refractaires," Rev. Hautes Temper. et Refract., Vol. 1, 1964, p 23.

41. A. T. Chapman and G. W. Clark, "Growth of UO_2 Single Crystals Using the Floating-Zone Technique," Journal of the American Ceramic Society, Vol. 48, 1965, p 494.

42. D. N. Hill, "Internal Zone Melting of Refractory Oxides Using Induced Eddy-Current Heating," Master's thesis in the School of Ceramic Engineering, Georgia Institute of Technology, 1969.

43. C. A. Tudbury, Basics of Induction Heating, Vol. 1, John F. Rider Publisher, Inc., New York, 1960.

44. B. Gayet, J. Holder, and G. Kurka, "Melting UO_2 by Direct High Frequency Induction," C. E. A., Direction des Materiaux et Combustibles Nucleaires.

45. D. K. Smith and C. F. Cline, "Verification of Existence of Cubic Zirconia at High Temperature," Journal of the American Ceramic Society, Vol. 45, 1962, p 249.

46. R. Roth, "Zirconia Reactions in Binary Oxide Systems," Journal of the American Ceramic Society, Vol. 39, 1956, p 196.

47. P. Duwez, F. H. Brown, Jr., and F. Odell, "The Zirconia Yttria System," Journal of the Electrochemical Society, Vol. 98, 1951, p 356.

48. S. C. Carniglia, S. D. Brown, and T. F. Schroeder, "The Equilibria and Physical Properties of Oxygen-Deficient Zirconia and Thoria," Journal of the American Ceramic Society, Vol. 54, 1971, p 13.

49. A. T. Chapman, J. Brynestad, J. C. Wilson, and G. W. Clark, "Redox Equilibria in Molten Uranium Dioxide," paper given at the Fall Meeting of the Nuclear Division of the American Ceramic Society, San Francisco, Calif., Nobember 1, 1973.